Li *et al. Biochar* (2026) 8:87
https://doi.org/10.1007/s42773-026-00593-0

Biochar

REVIEW

Open Access

Driving biochar applications via intrinsic redox superiority: electron transfer mechanisms, quantification, aging effects, and design strategies

Shasha Li[1], Zimeng Zhang[1], Yanling Ren[1], Fan Lü[2], Xiaoying Hu[1], Zhenhan Duan[1], Lili Yang[1], Jianwei Du[1,3], Pinjing He[2], Mingyang Zhang[1*] and Yong Wen[1,3*]

Abstract

Biochar, a carbon-rich product of biomass pyrolysis, has attracted attention for its applications in pollution control, soil amendment, and carbon sequestration. However, its large-scale application is hindered by its inherently lower surface area and conductivity compared to activated carbon or graphene, and by the added costs/pollution of post-modifications. Notably, the intrinsic advantages of biochar, particularly redox properties (i.e., electron exchange capacities, EEC) arising from redox-active moieties (RAMs), enable it to outperform other materials in facilitating electron transfer for pollutant degradation and energy recovery, thereby enhancing its competitive edge. Herein, we systematically review (i) the types and microspatial distribution of RAMs governing redox availability and spatial accessibility, which dominate the contribution of EEC in electron transfer; (ii) chemical, electrochemical, and microbiological techniques for quantifying EEC, highlighting methodological strengths, limitations, and interferences; (iii) the multifactorial impact of environmental aging on EEC, relating to long-term electron transfer performance; (iv) targeted strategies to enhance EEC, with precise tuning and trade-offs between performance and economic/environmental costs being recognized as current challenges. Future research perspectives are proposed to unveil electron transfer mechanisms controlled by redox potential and spatial accessibility behind different scenarios, refine the identification and visualization techniques of RAMs to assist mechanism interpretation and structure tuning, standardize EEC quantification protocols to eliminate interferences, monitor long-term performance changes, and regulate the internal elements in feedstocks through co-pyrolysis integrated with intelligent multi-objective optimization for targeted performance enhancement. By prioritizing the inherent redox properties of biochar, this work aims to guide sustainable, cost-effective strategies for maximizing its environmental utility.

Highlights

- The redox properties of biochar, outperforming other materials in electron transfer, enable large-scale application.
- Redox potential and spatial accessibility of RAMs probably affect electron transfer performance and quantitation.

*Correspondence:
Mingyang Zhang
kyuzmy@126.com
Yong Wen
wenyong@scies.org
Full list of author information is available at the end of the article

Springer

- Targeted enhancement of EEC and long-term performance of biochar in electron transfer during aging needs investigation.

Keywords Pyrochar, Aging, Biochar engineering, Electron donating/accepting capacities (EDC/EAC), Pseudocapacitance, Redox mapping

Graphical Abstract

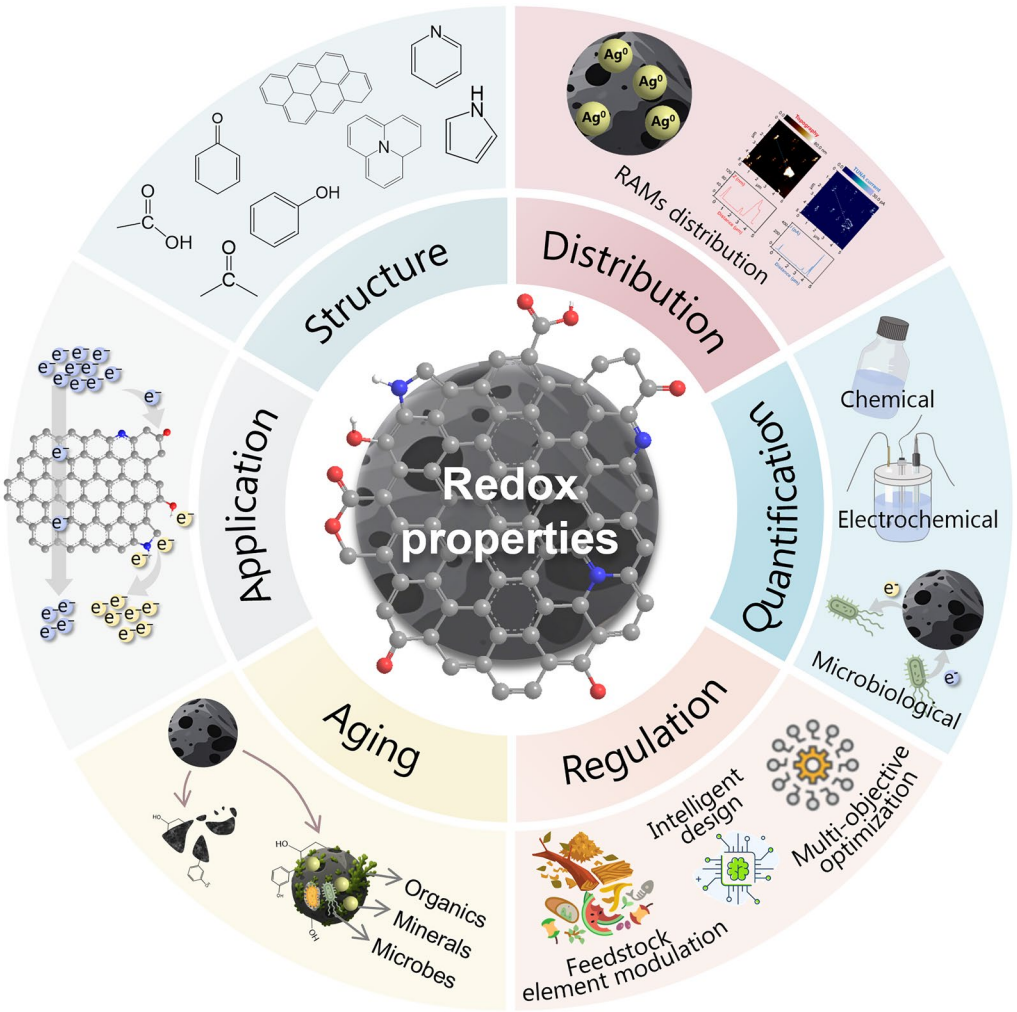

1 Introduction

Biochar is a carbon-rich material produced from the thermochemical decomposition of biomass in a low-oxygen atmosphere. With high carbon content, a porous structure, and abundant functionality, biochar has been considered "black gold" due to its promising applications in environmental remediation for pollution control and energy recovery, soil amendment to enhance fertility, and carbon sequestration to mitigate climate change (Tan and Yu 2023). However, the large-scale application of biochar is constrained by its intrinsic drawbacks, especially compared to other materials. For instance, the adsorption capacity of biochar for pollutant removal is often significantly lower than that of commercial activated carbon (Tan and Yu 2023) and resin (Marzbali et al. 2023), given that the specific surface area of biochar is generally lower (0–500 $m^2\ g^{-1}$ for biochar (Amen et al. 2020) vs. 500–3000 $m^2\ g^{-1}$ for activated carbon (Kah et al. 2017))

and resin possesses high inherent cation exchange capacity (Marzbali et al. 2023). Graphene-based cathode catalysts achieved higher power densities than biochar-based ones in microbial fuel cells, owing to their extensive surface area, high porosity, and high electrical conductivity, and graphene-based cathodes are even less expensive for field-scale reactors (Dhanda et al. 2023). Modification is widely used to enhance the functions of biochar, including activation with acids or alkalis, treatment with oxidants or reducing agents, coating with minerals or nanoparticles, and doping with heteroatoms (Wang and Wang 2019). Nevertheless, these modifications may also lead to structural instability, increased energy consumption, secondary pollution, and/or additional costs, thereby undermining cost-effectiveness and environmental sustainability (Zhang et al. 2022). Consequently, the insufficient intrinsic performance of pristine biochar, coupled with the additional cost and pollution associated with modification, undermines the competitiveness of biochar for lage-scale practical applications.

Then, what can we do to promote the competitiveness of biochar? Although biochar is highly tunable and can be engineered into multifunctional materials, with consideration of environmental and economic trade-offs, making good use of its inherent superior features, particularly the presence of heteroatoms and abundant functional groups, can be a promising way to promote its widespread application. Generally, biochar contains more heteroatoms (e.g., N, S, and mineral elements) and abundant functional groups, but a less ordered structure, lower conductivity, and lower surface area than other carbonaceous materials such as graphene, activated carbon, and carbon nanotubes (Qin et al. 2020). Heteroatoms in biochar predominantly exist within functional groups, which serve as key active sites facilitating electron transfer in the redox transformation of contaminants (He et al. 2022). Furthermore, the performance of biochar to facilitate microbial and abiotic electron transfer in pollutant removal, energy recovery, and photocatalytic CO_2 reduction was demonstrated to surpass that of other carbonaceous materials, including activated carbon, graphene, and carbon nanotubes (Li et al. 2024a; Chen et al. 2014; Prado et al. 2019; Wei et al. 2024b), and most minerals, such as magnetite, pyrite, and mackinawite (Ai et al. 2019, 2020). This advantage is closely linked to the superior redox properties of biochar, which are mainly dependent on redox-active moieties (RAMs), i.e., oxygenated or nitrogenated functional groups, persistent free radicals, and minerals (Yuan et al. 2022a; Cuong et al. 2021). Thus, the redox properties are promising to provide a competitive edge for biochar in various environmental applications.

This review aims to attract research attention to environmentally and economically sustainable targeted synthesis strategies to amplify the intrinsic electron-transfer performance of biochar and enhance its practical application feasibility. It does not reiterate topics that have been thoroughly covered by existing reviews, such as electron-donating and electron-accepting characteristics as a function of feedstocks and pyrolysis temperature (Tian et al. 2021), or the formation mechanisms of redox-active moieties and their applications in contaminant removal and microbial enhancement (Yuan et al. 2022a; Gao et al. 2023). In contrast, this review is distinctly focused on elucidating the roles and mechanisms of biochar in electron transfer, the underlying structure–property relationships, its long-term performance evolution during environmental aging, and targeted design strategies. Specifically, it focuses on: (i) revealing the essential definition under interdisciplinary elaboration; (ii) providing insights into the superior pollutant degradation performance of biochar predominantly governed by redox properties and their accessibility; (iii) analyzing RAMs and their microspatial distribution characteristics in biochar; (iv) comparing the advantages and limitations of chemical, electrochemical, and microbiological quantitative measurements and outlining key considerations during the quantification process; (v) summarizing the effects of environmental aging on the biochar structure and the possible resulting changes in redox properties. Targeted synthesis of biochar for redox properties was highlighted to employ low-pollution and cost-effective approaches through data-driven feedstock element modulation and biochar structural design. Finally, we propose that future research leverage the superiority of biochar in electron transfer by providing deeper insights into RAM accessibility and long-term structural evolution to support large-scale applications.

2 Definitions and interdisciplinary expressions of redox properties

Redox properties are intrinsic properties of diverse inorganics and organics, including minerals (Byrne et al. 2015; Shi et al. 2016), humic substances (HS) (Ratasuk and Nanny 2007), carbonaceous materials (Klüpfel et al. 2014), etc. Electron exchange capacities (EEC), electron storage capacities, electron transfer capacities (ETC), and pseudocapacitance were often used to express redox properties of biochar.

2.1 Electron exchange capacities

EEC, consisting of electron-donating and electron-accepting capacities (EDC and EAC), serves as a quantitative indicator of redox properties (Klüpfel et al. 2014; Saquing et al. 2016), also referred to as electron storage capacities. The measurement methodologies include chemical, electrochemical, and biological techniques (Klüpfel et al. 2014; Saquing et al. 2016; Xin et al. 2019; Prevoteau et al. 2016; Sun et al. 2018). Thus, EEC can be regarded as apparent redox properties influenced by the accessibility of different measurements. The EEC of biochar originates from abundant RAMs, such as quinone/hydroquinone and pyrrolic-N/pyridinic-N pairs, free radicals (Klüpfel et al. 2014; Ren et al. 2020; Yan et al. 2018; Zhong et al. 2019), and metals (Chacón et al. 2017).

2.2 Electron transfer capacities

ETC has also been referred to in the literature as the sum of EDC and EAC, which equals EEC. However, according to the literal meanings, electron transfer capacities should also include electrons transferred via electrical conduction, as well as those transferred via redox reactions. Therefore, in this article, electron transfer capacities refer to the total number of electrons transferred through both redox reactions and electrical pathways.

2.3 Pseudocapacitance

Pseudocapacitance is based on battery-like redox reactions and exhibits electrochemical behavior similar to that of a capacitor (Choi et al. 2020). It is primarily attributed to the presence of nitrogen and oxygen functionalities (Liu et al. 2019c), metallic oxides, and/or metals (Kalinke et al. 2021). Faradaic reaction-based pseudocapacitive energy storage and electrochemical double-layer capacitive energy storage constitute two main supercapacitor working mechanisms (Feng et al. 2019). Pseudocapacitance contains three main types: adsorption, redox, and intercalation pseudocapacitance. Redox pseudocapacitance, originating from the kinetically fast redox reaction between an electrode and the electrolyte, is conceptually equivalent to EEC (Srividhya and Ponpandian 2024).

3 Application advantages of biochar and the role of redox properties

When it comes to redox transformation and pollutant degradation, biochar has been reported to outperform other materials, such as graphite, activated carbon, and magnetite. This outstanding capability offers significant potential for the large-scale application of biochar.

3.1 Extracellular electron transfer

The conductivity and redox properties of materials were both demonstrated to facilitate extracellular electron transfer. Conductive materials, such as graphite, coke, and carbon cloth, performed better in facilitating organic degradation than non-conductive ones, such as gravel and polyester cloth, confirming the promoting function of conductivity (Prado et al. 2019). Biochar with higher redox properties remarkably accelerates methanogenesis (Yuan et al. 2018) and microbial reduction of ferrihydrite (Wu et al. 2017), verifying the function of EEC in electron transfer cycles. Biochar features graphitic structures and redox-active surface functional groups, which can mediate electron transfer through both electron-conducting and redox reactions (Sun et al. 2017, 2018). The redox-active biochar with lower conductivity (3.7×10^{-4} S cm^{-1}) was discovered to perform better in enhancing microbial extracellular electron transfer for biodegrading pollutants than highly conductive graphite (15.07 S cm^{-1}) and coke (0.38 S cm^{-1}) (Prado et al. 2019). Biochar with EEC exhibited more efficient electron transfer during anaerobic phenol/sludge degradation than granular activated carbon and graphite, which have higher conductivity but no redox activity (Li et al. 2021; Lü et al. 2020). Statistical correlation analysis reveals a relationship between biotic efficiency and EEC rather than conductivity, implying that EEC plays a dominant role in higher biodegradation efficiency. A recent study quantified the electron flux during anaerobic methanogenesis mediated by conductivity (1.0×10^{-8}–5.1×10^{-5} A) and EEC (2.5×10^{-3}–4.6×10^{-3} A), and the results unraveled the dominance of EEC in the tradeoff between conductivity and EEC (Xu et al. 2025).

However, it has also been reported that biochar is not comparable to granular activated carbon or magnetite in enhancing methanogenesis (Zhu et al. 2023). The divergence across publications can be due to the different performances of conductivity and EEC in various application scenarios. For instance, it has been found that redox-active biochar mainly enhances hydrolysis, acidogenesis, and hydrogenotrophic methanogenesis in anaerobic digestion, whereas conductive Fe_3O_4 or graphite primarily improves acetoclastic methanogenesis (Lü et al. 2020; Wang et al. 2023a). The difference between biochar and conductive materials is probably because conductors can only transfer electrons, while RAMs can also buffer extra electrons (Wang et al. 2023a). This can also explain why biochar exhibited positive effects under stressed conditions (electron deficiency) but competitive effects in well-operating scenarios (electron abundance) (Shao et al. 2019). Moreover, other factors will influence the role of EEC in biochar applications. For example, redox-active oxygenated functional groups, rather than redox

properties, are reported to correlate with methane production rates, and this was ascribed to the limited accessibility of the functional groups to microbes due to the presence of pores smaller than microbes (Ren et al. 2020). There should also be another form of accessibility arising from the redox potential of functional groups, as redox potential plays a crucial role in the energetic reward affecting reduction rates, extents, and final microbial growth yields (Levar et al. 2017). Nevertheless, the causes of the different effects of biochar across scenarios are still worth studying.

3.2 Catalytic abiotic electron transfer

Biochar has been found to eliminate kinetic hindrance and facilitate electron transfer between contaminants and reductants (Ai et al. 2019; Xu et al. 2019). The efficiency of biochar in facilitating abiotic electron transfer has been reported to be comparable to that of zero-valent iron, which is one of the current state-of-the-art reductant materials, and to exceed that of Cu(II), magnetite, pyrite, and mackinawite (Ai et al. 2019, 2020). Furthermore, carboxyl and carbonyl groups in biochar have been found to enhance photocatalytic conversion of CO_2 to CO by decreasing activation energies of CO_2 molecules, achieving a CO production rate more than 10 times higher than that of other advanced carbon materials (i.e., graphene and activated carbon) (Wei et al. 2024b). Both the RAMs and the conductive structure of biochar have been reported to facilitate abiotic electron transfer (Ai et al. 2019; Xu et al. 2019, 2013, 2010). The reactivity of biochar regarding the transformation of hexahydro-1,3,5-trinitro-1,3,5-triazine (RDX) by sulfides correlated with conductivity. In contrast, the transformation did not occur when RDX and sulfides were physically separated but electrically connected (Xu et al. 2013), indicating that conductivity positively contributed to electron mediation, but only possessing conductivity is insufficient. Moreover, biochar has been shown to participate in redox reactions, but oxygenated groups are not involved (Xu et al. 2013), suggesting the presence of other RAMs and that oxygenated groups likely fall outside the active redox potential range. Furthermore, another study reported that biochar could mediate the reduction of trichloroethylene by green rust, while highly conductive graphitic materials without EEC showed no enhancement effect, but the catalytic activity of biochar was still correlated with the graphitization degree (Ai et al. 2020). Both studies reveal the indispensable role of EEC and the contribution of conductive graphitic structure to the electron-mediating activity. However, similar to the biological redox reactions, the functioning electron-transferring structure was discovered to vary with reaction types, as electrons for the reduction of 1,1-dichloro-2,2-bis(4-chlorophenyl)ethylene and nitroglycerin were conducted by graphitic structure, but those for 1,1-trichloro-2,2-di(4-chlorophenyl)ethane and 1,1-dichloro-2,2-bis(4-chlorophenyl)ethane were mediated by RAMs through pre-reacting with the reductants (Ding and Xu 2016; Xu et al. 2010). This is probably determined by the redox potentials of reductants and RAMs, that is, only when the redox potential allows reactions between RAMs and reductants can EEC participate in electron transfer.

On the other hand, biochar can also activate O_2 and peroxides (including H_2O_2, peroxymonosulfate (PMS), peroxydisulfate (PDS), and peracetic acid, etc.) to form reactive oxygen species (ROS) (including hydroxyl radical (•OH), superoxide anions ($O_2^{\bullet-}$), hydrogen peroxide (H_2O_2), sulfate radicals ($SO_4^{\bullet-}$), etc.) and degrade organic contaminants via radical pathways, or facilitate degradation of organic pollutants via non-radical pathways including singlet oxygen ($^1O_2$), surface electron transfer, and surface activated complex (Zhao et al. 2021; Wang et al. 2022a). Furthermore, it is reported that dissolved biochar can facilitate ROS production by promoting the growth of bacteria, as the total abundance of bacteria that mediate ROS production capacities by releasing nicotinamide adenine dinucleotide (NADH) is significantly positively related to the contents of $O_2^{\bullet-}$ and H_2O_2 (Yang et al. 2025). The 30-min •OH generation rate from biochar (9.5 ± 0.3 nM min^{-1}) was reported to surpass that of dissolved organic matter (2.8 nM min^{-1}) and pyrite (0.7 nM min^{-1}) (Li et al. 2024c), demonstrating the superiority of biochar over other activators in producing ROS. Similarly, as evidenced by the correlation between EEC and H_2O_2 production, the EEC of biochar was shown to be critical for activation (Li et al. 2024c). During these activation processes, persistent free radicals (PFRs), oxygenated functional groups, redox metals/metal oxides, carbon defects, oxygen vacancies, and heteroatoms such as N, S, and B will act as electron donors (Wang et al. 2022a; Ji et al. 2025; Zhao et al. 2021). The graphitic structure can serve as an electron-transfer bridge (Du et al. 2020). Nonradical pathways have anti-interference ability and broad adaptability to their surroundings, and can prevent radical self-quenching and maximize the oxidizing capacity of oxidants compared to radical pathways (Wang et al. 2023b). Therefore, it is possible to promote nonradical pathways to become the dominant electron-transfer mechanism by altering the electronic structure of biochar through tuning its graphitization degree and oxygenated functional groups (Wang et al. 2023b).

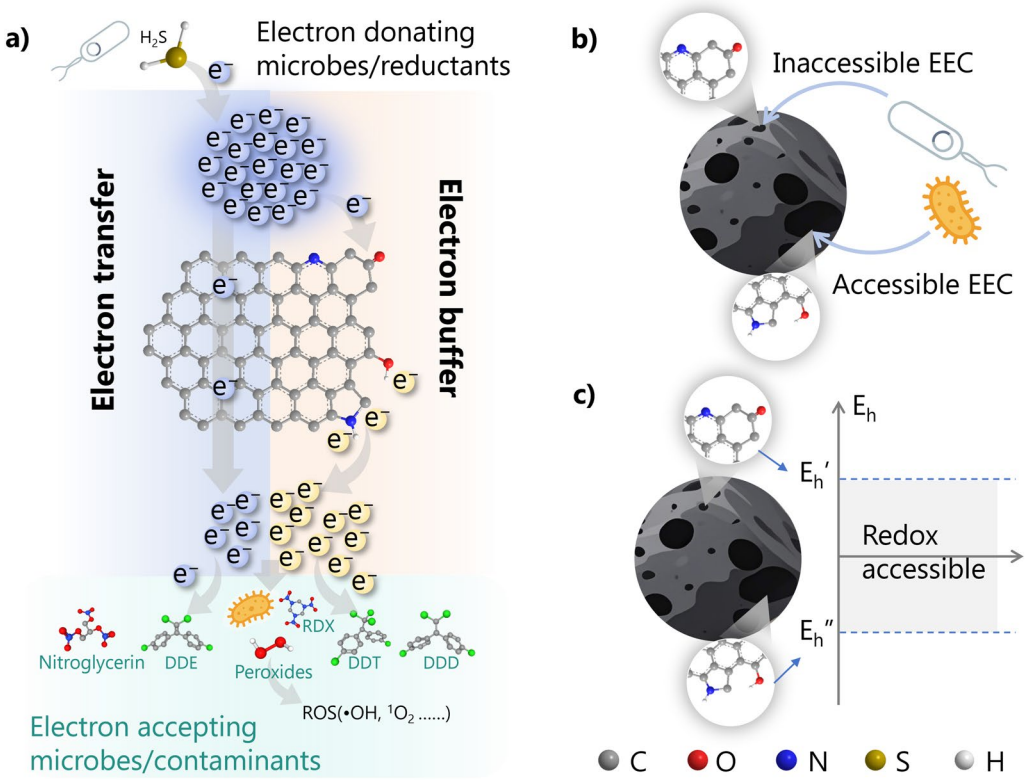

Fig. 1 The roles **a** and accessibility **b**, **c** of EEC in electron transfer of biochar

3.3 Perspectives

In summary, the superior performance of biochar over conductive materials such as graphite and activated carbon in facilitating biological and abiotic electron transfer processes is primarily attributed to the pivotal role of its EEC (Fig. 1). Coupled with its low cost and extensive availability, biochar shows potential for large-scale application in the redox degradation of pollutants. Nevertheless, the contributions of biochar's conductivity and redox properties to electron transfer processes vary with scenario, and the underlying regulatory mechanisms remain incompletely elucidated. The redox potential difference between RAMs in biochar and electron-transfer partners (e.g., microorganisms, oxidants, reductants) is deduced to be the dominant factor in determining whether EEC can contribute to electron-transfer processes (Fig. 1).

4 Identification and microspatial distribution of RAMs

Redox properties are derived from the existing redox-active moieties (RAMs). Hence, recognizing the molecular structure (related to redox potential) and distribution (related to spatial accessibility) of redox sites should be fundamental to exploring the mechanisms of chars in various scenarios. RAMs identified by previous publications are illustrated in Fig. 2a.

4.1 Redox-active moieties

4.1.1 Organic functional groups

Quinone/hydroquinone pairs and semiquinone radicals have been the most widely reported redox sites in biochar (Klüpfel et al. 2014; Zhong et al. 2019; Yuan et al. 2018; Zhang et al. 2019c; Ai et al. 2020) and hydrochar (Yan et al. 2018; Ren et al. 2020). Moieties other than quinoid groups in biochar have been recognized as potentially redox-active, mainly oxygenated and nitrogenous groups (Liu et al. 2019a). Conjugated π-electron systems can be electron-accepting moieties in high-temperature pyrolytic chars in light of the consistent trend of biochar composition and EAC (Klüpfel et al. 2014), and the conjugated π-electron systems were found to contribute to EDC as well (Zhang et al. 2018). Lactonic groups were linearly correlated to EEC in pyrolyzed hydrochar (Saha et al. 2019) and EDC in biochar (Zhang et al. 2018). Carboxyl and carbonyl groups were identified as electron acceptors using multiple linear regression (Zhang et al. 2019c). Conversely, carboxyl groups were eliminated from moieties contributing to capacitance by comparing capacitance before and after their removal

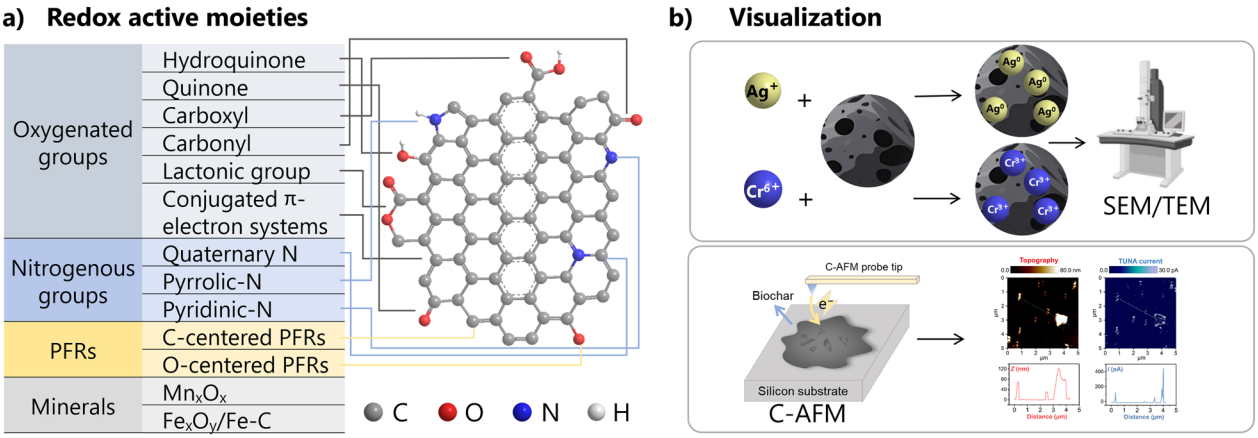

Fig. 2 **a** RAMs and **b** their visualization methods (Xin et al. 2020; Liu et al. 2019b; Li et al. 2022)

(Bleda-Martínez et al. 2006). N-dopants will reduce the electron density on the carbon surface, thereby increasing electron acceptance (Yang et al. 2017). Graphitic N (also called quaternary N) could serve as an electron donor based on the lone pair of electrons (Yu et al. 2018) and assist electron transport in the carbon (Sevilla and Mokaya 2014), while negatively charged pyrrolic-N and pyridinic-N contribute to pseudocapacitive (Sevilla and Mokaya 2014), which refers to the ability to store electrical energy through faradaic reduction–oxidation reactions (i.e. EDC and EAC) (Chacón et al. 2017).

4.1.2 Persistent free radicals

PFRs present in chars are special RAMs, which have been observed to mediate redox reactions by donating and accepting electrons directly, as well as indirectly inducing the production of ROS (i.e., $\bullet O_2^-$, H_2O_2, and $\bullet OH$, etc.) (Zhong et al. 2019; Tian et al. 2021). The presence of PFRs in biochar was first reported in 2014, but the PFR species were not clarified (Fang et al. 2014). The types of PFRs are often classified into C-centered PFRs (g-factor < 2.0030), C-centered PFRs with an adjacent oxygen atom (g-factor in 2.0030–2.0040), and O-centered PFRs (g-factor > 2.0040) based on the g-factor (Zhong et al. 2019; Yuan et al. 2022b; Tian et al. 2021). But g-factor is also influenced by substituents and matrix interactions (Xie et al. 2024), which can lead to deviations in PFR identification. For example, nitrogen dopants in BC alter the charge of the carbon matrix and PFRs (Zhu et al. 2020). It was reported that PFR intensities were correlated with C=O and aromatic C=C groups, and C=O (possibly aldehydes, aromatic ketones, and quinones) contributed 49.3% of PFRs in lignocellulose-derived biochar (Tao et al. 2022). Furthermore, other fractions of biochar, such as metals and phenolic compounds, can influence the concentrations and types of PFRs (Fang et al. 2015).

4.1.3 Other RAMs

The redox metals in biochar also contribute to the enhancement of electron transfer. It is confirmed that pre-loading of redox-active metals (such as Fe and Mn) can enhance redox properties (Chacon et al. 2020). The transition of Fe morphology and crystallinity will alter redox properties of the Fe-modified biochar, as proved by the observation that the contents of amorphous ferrous minerals were positively correlated to EDC (Xu et al. 2022). Moreover, Fe can probably react with carbon and induce the formation of oxygenated moieties, such as hydroxyl and quinoid (Xu et al. 2022). It was reported that intrinsic Mn and Zn in biomass facilitate the generation of RAMs, e.g., PFRs, oxygenated moieties, and graphite-like structures in biochar, thus enhancing electron-donating and electron-accepting processes (Wang et al. 2022d). However, Zn was also observed to inhibit the formation of PFRs, carboxyl, and benzoquinonyl groups but increase phenol groups (Mai et al. 2017; Huang et al. 2023). This disagreement may result from the different types of PFRs. Besides, several typical structures can enhance electron-transfer processes by changing the accessibility or electronic characteristics. For example, graphitic carbon can act as a conductor and enable relatively long-distance electron transfer, increasing the accessibility of redox-active electron donors and acceptors (Sun et al. 2017), while some electrochemically inert oxygenated functional groups can promote pore access and surface utilization by increasing wettability (Liu et al. 2019c). g-C_3N_4 nanodots and ultra-thin g-C_3N_4 nanoflakes can enhance the utilization of electrons and holes by adjusting intrinsic bandgap and surface electronic characteristics (Zhu et al. 2025).

4.1.4 Limitations and perspectives

The identification of RAMs is often based on statistical relevance, including similar trends (Klüpfel et al. 2014), single-factor linear regression (Zhu et al. 2020; Saha et al. 2019; Wu et al. 2017; Yan et al. 2018), multiple-factor linear regression (Zhang et al. 2019c, 2018), and partial least squares regression (Li et al. 2020). However, apart from oxygenated quinoid groups and nitrogenated pyrrolic/pyridinic-N moieties, the inconsistencies in the recognition of the other redox moieties in chars appeared in the research mentioned above (such as lactonic groups and carboxyls) (Klüpfel et al. 2014; Zhang et al. 2018, 2019c; Saha et al. 2019; Li et al. 2020), which might result from the mathematical methodology of relevance based on finite statistics with the lack of experimental observations. Besides, the redox potential of functional groups would be influenced by the biochar matrices to which they are bonded. The limits of characterization techniques for functional groups would lead to variations in the measured contents. For example, XPS can only measure 10-nm depth from the material surface, and it cannot distinguish aliphatic and aromatic forms of the functional groups (e.g., quinoid C=O and aliphatic C=O) (Chacon et al. 2020). Although RAMs are generally recognized as oxygenated and nitrogenous functional groups or radicals in chars (Klüpfel et al. 2014; Zhu et al. 2020), the inconsistent identification of RAMs spurs further research demand to identify them through experimental observation.

4.2 Microspatial distribution of RAMs in biochar

To be noted, structural properties, such as porosity, which are expected to affect the spatial accessibility of the RAMs, are often not included in the determinants of redox properties. One of our previous publications (Li et al. 2020) incorporated specific surface area into the electron-transfer factors and quantified the contributions of each component using partial least squares regression. The results showed that the surface area would limit the apparent ESC despite the evident presence of redox-active nitrogenated groups in casein-derived biochar. At the same time, the large surface area also induced both high EDC and EAC of starch-derived biochar pyrolyzed at 700℃ with relatively lower contents of functional groups than biochar pyrolyzed at lower temperatures. Thus, the variation in RAM distribution induced by structural characteristics plays a significant role in the accessibility of RAMs during the electron-donating and -accepting processes. Meanwhile, when investigating the electron transfer mechanisms of chars, redox properties vary with the observed RAMs (Wu et al. 2017; Wang et al. 2019a; Zhang et al. 2019b), but Ren et al. (2020) observed that it was not the redox properties but the surface oxygenated groups that correlated with methane production rates. This indicates that some of the present groups are unavailable to provide electrons or serve as electron sinks. Consequently, recognizing the distribution of RAMs is crucial for distinguishing the functional part and enhancing it in practical applications.

It has been widely recognized that redox sites caused by heteroatoms are reasonably supposed to be bonded to carbon atoms on the edge surface or neighboring structural defects (Inagaki et al. 2010). However, the heterogeneity and irregular morphology of biochar make it challenging to ascertain the distribution of RAMs. Two main categories of methodologies have been reported to visualize the distribution of RAMs (Fig. 2b). One is to use redox-active metal ions as markers. Ag^+ was used to tag the reductive moieties, and the reduced Ag^0 nanoparticles can be visualized by microtome imaging to show the distribution of electron-donating moieties (Xin et al. 2020). The distribution of reductive moieties was also visualized using procedures in which Cr(VI) was first adsorbed and diffused into biochar, then reduced to Cr(III), followed by confocal micro-X-ray fluorescence imaging (Liu et al. 2019b). The other methodology is to combine physical, optical, and electrochemical microscopes. A conductive atomic force microscope (C-AFM) was used for simultaneous in situ observation of topographic and electrochemical properties at the nanoscale, and SEM–EDS/Raman were further used to characterize the physicochemical structure, thereby enabling the observation of electroactive moieties and a direct link between structure and electrochemical properties (Li et al. 2022). Furthermore, a multi-exfoliation method and characterization of colloidal biochar from different layers were proposed to reveal the spatial distribution of RAMs in biochar particles, which will influence long-term functional sustainability of bulk biochar (Li et al. 2023), as biochar will undergo physical disintegration into fragments and form colloids when entering the environment (Wang et al. 2020a, 2019b).

Nevertheless, the visualization methods for the microspatial distribution of RAMs still have some limitations. For the tagging method, the moieties that can be visualized are limited by the redox potential range of the markers, and the positioning of the markers will likely be influenced by adsorption properties. For the microscopic method, a limitation lies in its inability to distinguish between conductive moieties and RAMs, and the applicability of C-AFM is primarily determined by the surface flatness of biochar particles. For the characterization of spatial distribution, the exfoliation process is likely to alter the surface of biochar colloids exfoliated from bulk biochar, which would lead to some deviations. Therefore, the microspatial distribution of RAMs in biochar, which

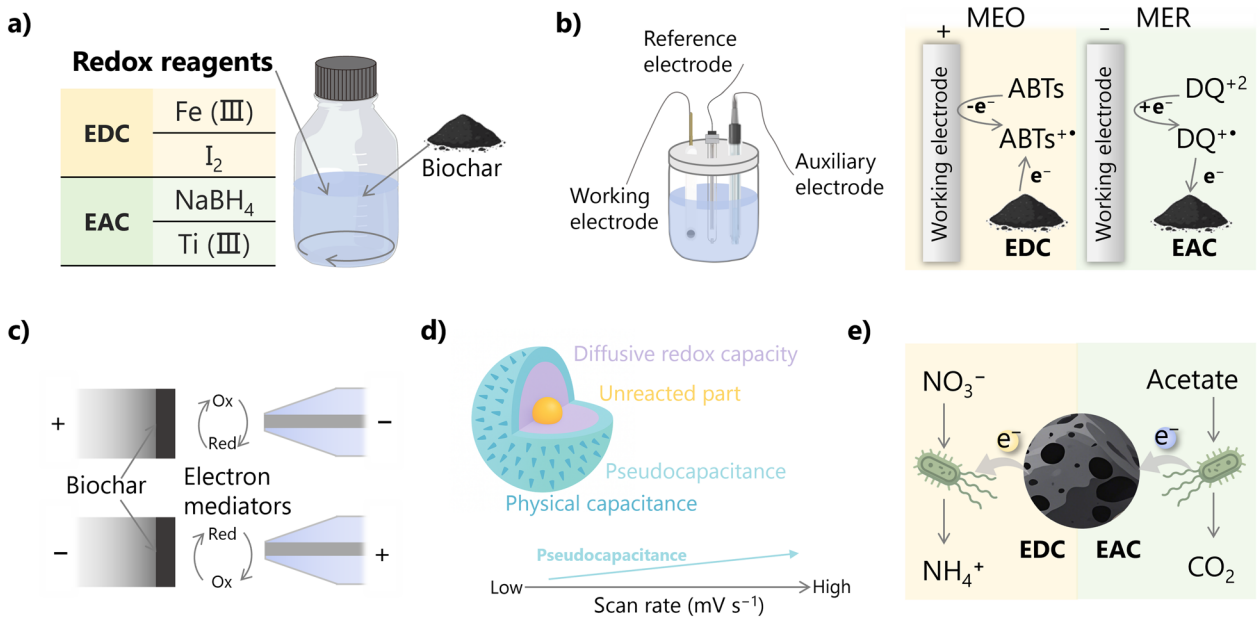

Fig. 3 Illustration of chemical, electrochemical, and microbiological quantitative methods for EEC

governs the availability associated with redox potential and spatial accessibility, still requires further investigation of visualization methods.

5 Quantitative measurements of redox properties

5.1 Chemical, electrochemical, and microbiological quantitative methods

5.1.1 Chemical measurement

Specific redox reagents with known standard redox potentials are usually utilized for chemical measurements of redox properties. Oxidants (frequently chosen as Fe(III) species (Bauer et al. 2007) and I_2) (Yan et al. 2018) and reductants (such as $NaBH_4$ (Mai et al. 2017), Ti(III) species (Xin et al. 2019; Saha et al. 2019)) are employed for quantifying EDC and EAC, respectively (Fig. 3a). Briefly, precisely weighed chars are dispersed into a solution with a specific concentration of a redox reagent, which has been purged with N_2 to eliminate oxygen and buffered to a neutral pH. The acquired suspension is tightly sealed or transferred to an anaerobic glovebox and subsequently agitated in a shaker for an equivalent time until equilibrium is reached, after which the residual redox reagents are determined. EEC (EDC plus EAC, mmol e^- g^{-1} char) is calculated using the amount of electrons transferred by consumed redox reagents accordingly (Eq. 1).

$$\text{EDC or EAC} = n_e \times (C_i - C_e) \times V/M \quad (1)$$

where n_e (mmol e^- mol^{-1}) means the number of electrons transferred per mol oxidant or reductant, C_i and C_e (mol L^{-1}) are the concentrations of oxidant or reductant in the initial and the equilibrium solutions, respectively, V (L) is the volume of the redox solution, and M (g) is the weight of the tested char.

5.1.2 Electrochemical measurement

Cyclic voltammetry (CV) and chronoamperometry (CA) are primarily used for electrochemical measurements of EEC. As biochar is granular and largely insoluble, achieving redox equilibria between biochar and working electrodes in electrochemical measurements is challenging. Two main strategies are often taken to overcome this. One is to establish direct contact between biochar and the working electrode, or to use biochar as the working electrode. The other is to use dissolved redox mediators to facilitate electron transfer and redox equilibration between the working electrode and biochar (Sander et al. 2015).

1) Methods derived from CA

Mediated electrochemical oxidation (MEO) and reduction (MER) based on CA are the most commonly used electrochemical methods (Klüpfel et al. 2014), in which a three-electrode (i.e., a working electrode, a reference electrode, and an auxiliary electrode) test system is required. The electrolyte should be purged with N_2 to eliminate oxygen and buffered to a neutral pH before the test (Fig. 3b). A certain amount of oxidizing (in MEO) or reducing (in MER) mediator (soluble and reversibly accelerates electron transfer between the biochar and the

electrode) is added to the electrolyte (Sander et al. 2015), and a constant voltage is applied to the working electrode to oxidize or reduce the medium. When the recorded current becomes stable, a certain amount of fine biochar suspended in anoxic buffer solution (the same as the electrolyte) can be added into the electrolyte separated from the auxiliary electrode by a porous glass frit. The EDC and EAC can be calculated by integrating the resulting oxidative and reductive current peaks, respectively (Eq. 2).

$$\text{EDC or EAC} = \frac{\int \frac{I}{F} dt}{M} \tag{2}$$

where I (A) is the baseline-corrected current, F is the Faraday constant, t (s) is the equilibration time, and M (g) is the weight of added char.

A four-electrode configuration and dual-interface electron transfer detection (referred to as the four-electrode method) were proposed to distinguish electron transfer by functional groups from that by carbon matrices and quantify their relative contribution to total electron transfer (Fig. 3c) (Sun et al. 2018). A four-electrode setup includes two working electrodes (a biochar electrode made by immobilizing biochar thin sheets onto a glassy carbon disk electrode, and a platinum microelectrode), a counter electrode, and a reference electrode. The four-electrode method works on the basis of electron transfer processes across two working electrode–solution interfaces (Sun et al. 2018). (Dimethylaminomethyl)ferrocene (FcDMAM) is used as a mediator because it can oxidize hydroquinone/phenol groups, but not reduce quinone groups. The platinum electrode is polarized (30 min) to +0.65 V (vs. the standard hydrogen electrode, SHE) to oxidize $FcDMAM^0$ to $FcDMAM^+$, then −0.5 V (vs. SHE) is continuously applied to the biochar electrode to measure total electron transfer by biochar. Conversely, the applied potentials for the biochar and platinum electrodes were +0.65 and −0.5 V to measure electron transfer through carbon matrices. The transferred electron can be calculated by integration of the current response, and the electrons transferred by functional groups can be calculated by subtracting those transferred by carbon matrices from the total electron transfer.

2) Methods derived from CV

CV is another electrochemical method for measuring EEC (Prevoteau et al. 2016). Similarly, all manipulations need to be taken in an anaerobic workstation, and all the used solutions and biochar were pretreated to eliminate the influence of oxygen. The ground biochar was reacted for a specific time (approximately 20 days) in buffered oxidative (ferricyanide) and reductive (neutral red) solutions, respectively, before the CV tests for EDC and EAC. CV was performed from −0.5 V to +0.7 (vs. Ag/AgCl electrode) at 50 mV s^{-1}. The EDC and EAC can be calculated using the background-subtracted limiting current density, whose absolute value is proportional to the total ferrocyanide and neutral red concentrations, respectively.

CV is also recognized as a feasible electrochemical technique for quantitatively determining pseudocapacitance (Fig. 3d) (Pu et al. 2021). The current in the CV test at a given potential is composed of physically capacitive current, pseudocapacitive current, and diffusive current. Both diffusive and pseudocapacitive currents originate from Faradaic reactions, distinct from physical capacitance (double-layer capacitance), where charge is stored through physical interactions at a rough surface. Pu et al. (2021) promoted a method to calibrate physical capacitance, pseudocapacitance, and diffusive capacity separately, which involves de-polarization, de-residual, and de-background, as well as non-linear fitting calculation, to calculate the pseudocapacitance contribution (Eq. 3). The de-polarization treatment is used to eliminate potential offsets, mainly caused by ohmic resistance, while the de-residual calibration is intended to alleviate the residual current when the scan direction is reversed.

$$I' = k_1' v + k_1'' v + k_2 v^{0.5} \tag{3}$$

where I' represents current after de-background, k_1' k_1'' k_2 are three variables, and v is the scan rate. Then, the variables at each potential can be calculated using the final calibrated current and scan rate, and integrating them can obtain the final physical capacitance, pseudocapacitance, and diffusive contribution separately.

5.1.3 Microbiological measurement

Microbiological measurement methods can be used to determine the bioavailable EEC of biochar (Fig. 3e) (Saquing et al. 2016). *Geobacter metallireducens* (GS-15, ATCC 53774) is selected as the microbe because it is not able to utilize H_2 as an electron donor but can use humic acid as both an electron acceptor and a donor. Biochar needs to be pre-oxidized and then incubated with a certain amount of sodium acetate in an anoxic medium, during which GS-15 oxidizes acetate to CO_2. After acetate oxidation, the biologically reduced biochar is separated and washed for subsequent nitrate-reduction experiments, during which GS-15 reduces nitrate to ammonium. The incubation medium and biochar are N_2/CO_2-purged before use, and the experiments are conducted in a glovebox. Biochar serves as the sole electron acceptor and donor of GS-15 for acetate oxidation and nitrate reduction.

$$EDC\ or\ EAC = n_e \times |C| \times V/M \quad (4)$$

where n_e (mmol e^- mol^{-1}) is the number of electrons transferred per mol of acetate or ammonium. C (mol L^{-1}) is the difference in concentration of acetate or ammonium between the initial and the final solutions, respectively. V (L) is the volume of the solution, and M (g) is the weight of the tested biochar.

a) Chemical measurement: dispersing biochar in an oxygen-free, buffered reagent solution of redox reagents with known standard potentials, agitating until equilibrium, and then calculating EEC by quantifying the remaining reagent. Oxidants such as Fe(III) species or I_2 are used for EDC, and reductants such as $NaBH_4$ or Ti(III) species for EAC. b) Mediated electrochemical measurement: employing an oxidizing (usually 2,2′-Azino-bis(3-ethylbenzothiazoline-6-sulfonic acid) diammonium salt, ABTs) or reducing (usually 1,1′-ethylene-2,2′-bipyridinium dibromide monohydrate, DQ) mediator in a three-electrode system under a constant applied voltage, adding biochar suspension after the current becomes stable, and calculating EDC or EAC by integrating the current response over time after biochar addition (Klüpfel et al. 2014). c) Four-electrode method: employing a dual-working-electrode setup with a specific mediator, i.e., (Dimethylaminomethyl)ferrocene (FcDMAM), and alternating polarization to distinguish and quantify electron transfer contributions from functional groups versus the carbon matrix. The electron transfer attributed to functional groups is calculated by subtracting the matrix contribution from the total electron transfer (Sun et al. 2018). d) Pseudocapacitance quantification: distinguishing and quantifying the contributions of physical capacitance, pseudocapacitance, and diffusion-controlled processes in biochar through current deconvolution and non-linear fitting (Pu et al. 2021). e) Microbiological measurement: employing *Geobacter metallireducens* (GS-15) to determine the bioavailable EEC of biochar by utilizing biochar as the sole electron acceptor during acetate oxidation and as the sole electron donor during nitrate reduction, with electron transfer quantified via metabolite concentration changes(Saquing et al. 2016) (Fig. 4).

5.2 Considerations for different measurement methods

Accuracy, stability, and convenience are the crucial criteria for selecting testing methods. In this section, we summarize the strengths and limitations of these methods, along with the considerations required for each approach. The EDC and EAC of biochar tested by different methodologies are summarized in Table 1 and Fig. 2. Among previous publications, chemical and electrochemical methods (MEO and MER) were most commonly used due to their reproducibility and convenience.

5.2.1 Chemical measurement

When using chemical measurements, it is accurate to recognize equilibrium and flexible to adjust the reaction time before equilibrium by changing the concentration of redox agents. However, the following items should be taken into consideration. 1) Redox potential of employed reagents. As illustrated in Table 1, the redox reagents have different E_h values, which determine the reacting possibility of RAMs across different redox potential ranges, so that the measured EDC or EAC would vary with the redox reagents. Thus, the redox potential of a redox reagent for redox property measurement should cover the redox potential range of existing RAMs. 2) pH. It was proposed that increasing pH would decrease the reduction potential of humic acid (HA), as a result of proton uptake during the electron-transfer process (Aeschbacher et al. 2011). Meanwhile, the predominant RAMs responsible for oxidation transition from phenolic−OH and semiquinone-type PFRs to semiquinone-type PFRs and quinoid C=O groups with pH changing from acidic to alkaline (Zhong et al. 2019). Consequently, pH-stat acid titration or buffer solution with pH monitoring should be used to maintain pH stability during the measurement. 3) Adsorption of redox reagents. Biochar is a carbonaceous material with specific adsorption capacity due to the presence of oxygenated and nitrogenated functional groups and porous structure (Su et al. 2024). Adsorbed redox agents are counted in, leading to the measured EEC higher than the actual value. In particular, biochar with a distinct adsorption capacity will induce different system errors and make it hard to compare the EEC among them.

5.2.2 Electrochemical measurement

Redox mediators, equilibration duration, and perturbation are the critical factors of MEO and MER. Redox mediators are intended to facilitate rapid redox equilibration between the electrode and the analyte via electron transfer. Thus, mediators should meet the following requirements: 1) The electron transfer by mediators must be fully reversible. 2) Mediators should have defined apparent standard redox potentials and known numbers of electrons transferred during reduction/oxidation. 3) Mediators must not degrade during the measurement (Sander et al. 2015). In the previous publications, 2,2′-Azino-bis(3-ethylbenzothiazoline-6-sulfonic acid) diammonium salt (ABTS, $E_H{}^{0'} = +0.70$ V vs. SHE) and 1,1′-ethylene-2,2′-bipyridinium dibromide monohydrate (diquat, $E_H{}^{0'} = -0.35$ V vs. SHE) are the mainly used oxidative and reductive mediators, respectively. Moreover,

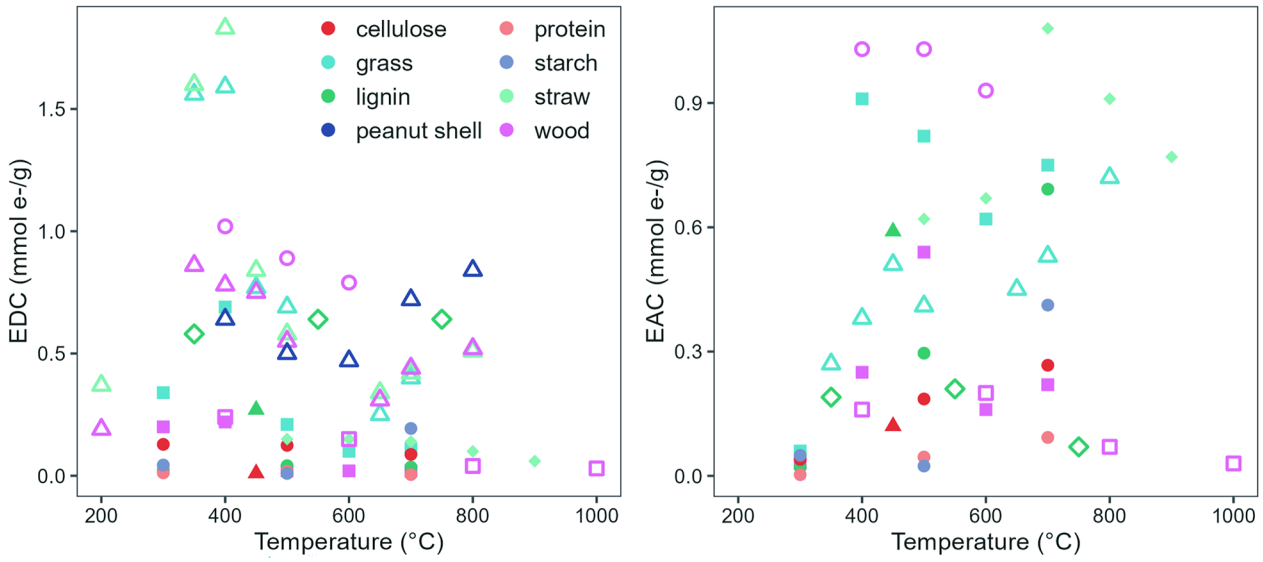

Fig. 4 EDC **a** and EAC **b** values of biochar determined using MEO and MER in previous publications (Klüpfel et al. 2014; Xin et al. 2021; Yu et al. 2022; Chacon et al. 2020; Sathishkumar et al. 2020; Li et al. 2020)

Table 1 EEC values of chars determined using chemical and microbiological measurements

Producing method	Feedstock	T (℃)	Redox reagent	E_h (V)	pH	Duration	EEC (EDC, EAC) (mmol e^- g^{-1})	Ref
HC	Wheat straw/grass	240	I_2	+0.53	7.01(buffer)	5–10 h	0.4^{D}	(Yan et al. 2018)
	Lignin	240	Fe(III)	+0.77	2	96 h	6.41^{D}	(Mai et al. 2017)
			I_2	+0.53	7 (buffer)	30 min	1.02^{D}	
			$NaBH_4$	−1.24	12	Equilibration	0.36×10^{3A}	
			$NaBH_4$	−1.24	12	Titration	0.98^{A}	
	Cellulose	240	Fe(III)	+0.77	2	96 h	0.45^{D}	
			I_2	+0.53	7(buffer)	30 min	0.30^{D}	
			$NaBH_4$	−1.24	12	Equilibration	0.47×10^{3A}	
			$NaBH_4$	−1.24	12	Titration	0.49^{A}	
	D-xylose	240	Fe(III)	+0.77	2	96 h	0.56^{D}	
			I_2	+0.53	7(buffer)	30 min	0.14^{D}	
			$NaBH_4$	−1.24	12	Equilibration	0.22×10^{3A}	
			$NaBH_4$	−1.24	12	Titration	0.01^{A}	
HC220-PY	Hardwood	400	Ti(III) citrate, Dissolved oxygen	−0.36, +0.80	6.4	72h	3.25	(Saha et al. 2019)
		500					2.84	
		600					2.32	
PY	Hardwood	500	Dithionite	−0.43	6.4	12 h	5.08^{A}	(Xin et al. 2019)
			Ti(III) citrate	−0.36	6.4	2 d	3.83^{A}	
			$[Fe(CN)_6]^{3-}$	+0.43	7.0	1 d	2.07^{D}	
	Yellow wood	550	Ti(III) citrate, Dissolved oxygen	−0.36, +0.80	6.4	72h	4.11	(Xin et al. 2021)
	Cellulose	450					1.62	
	Xylan						1.07	
	Lignin						2.04	
	Pine wood						1.12	
	Hard wood	550	NO_3^-	Microbiological	6.9	6 d	0.83	(Saquing et al. 2016)
			Acetate				0.77	

The producing methods (HC, PY) represent hydrothermal carbonization and pyrolysis, respectively. The suffixes of figures (^{A}, ^{D}) in the EEC column represent EAC and EDC, respectively, and figures without suffixes represent EEC

Table 2 Summary of chemical, electrochemical, and microbiological measurements

Measurement	Advantage	Disadvantage	Detection range	Duration	Applicable scenario
Chemical method	High accuracy in identifying reaction equilibrium	Influenced by the E_h of redox reagents and the adsorption of redox reagents to biochar	Dependent on the redox potential of redox reagents (usually −1.24–+0.77 V)	Several hours to days	Imitating the contribution of EEC to abiotic electron transfer
Mediated electrochemical method	Faster than other measurements; Allowing real-time monitoring	Lacking criteria for determining equilibrium duration;Vulnerable to stirring and biochar addition operations	Dependent on the redox potential of redox mediators (−0.35–+0.70 V)	Several minutes to hours	Rapid screening and comparison among different chars
Microbiological method	Distinguishing bioavailable EEC; More relevant to actual biogeochemical processes	Only applicable to *Geobacter metallireducens* that cannot utilize H_2	Dependent on the redox and spatial accessibility of microbes	6 days	Assessing the contribution of EEC to microbiological metabolism

experimental observations show that the response current caused by added biochar will approach the baseline current indefinitely but remain above it. Hence, the determination criteria for equilibration duration are essential, as the integration width can affect the calculated results for transferred electrons. Besides, the physical and oxygen perturbations caused by magnetic stirring and biochar addition operations also need to be controlled and consistent among different tests. As for the two methods derived from CV, the method to calculate pseudocapacitance has not been used in environmental and geochemical fields, so the applicability and accuracy of the fitting method to biochar still needs to be further validated, while for the other one using current density, difference between the current density in the presence of char and without char is only proximately 5% of the fundamental signal change, which might induce relatively larger system error.

5.2.3 Comparisons of different measurements

MEO and MER take a shorter time to determine EEC than the chemical method (Xin et al. 2021), and make it possible to monitor the process of redox reactions through real-time recorded current to recognize abnormal tests. However, as shown in Table 1 and Fig. 2, the reported EDC and EAC values of biochar determined by MEO and MER fall in the range of 0–2 mmol e^- g^{-1} and 0–1.2 mmol e^- g^{-1}, respectively, while the EDC determined using chemical measurement can reach 6.41 mmol e^- g^{-1}, and the EAC can reach 5.08 mmol e^- g^{-1} or even more (470 mmol e^- g^{-1}). This can be ascribed to two determinants: 1) The reaction duration. For example, EAC of the same hydrochar, determined using $NaBH_4$ as the reductive agent, can differ by hundreds to thousands of times between titration and equilibration methods (Mai et al. 2017). And the EDC value of the same biochar, detected after 20-day mixing with the oxidative agent (Fe(III)), was observed to be one to two orders of magnitude higher than that obtained after 1-h equilibration (Prevoteau et al. 2016). Both observations indicate that the spatial accessibility of RAMs controlled by pore diffusion (Xin et al. 2021) will influence the apparent redox properties, i.e., EEC. 2) Redox potentials of redox agents. As shown in Table 1, for the same biochar and chemical measurement of equilibration, the higher EDC (6.41 mmol e^- g^{-1} vs. 1.02 mmol e^- g^{-1}) (Mai et al. 2017) and EAC (5.08 mmol e^- g^{-1} vs. 3.83 mmol e^- g^{-1}) (Xin et al. 2019) accompanies the higher $|E_h|$ of redox agents (0.77 V of Fe(III) vs. 0.53V of I_2, −0.43 of Dithionite vs. −0.36 of Ti(III) citrate). It has been proven that the EAC obtained by the chemical method and MER are correlated and can be estimated by each other, when the E_h of redox agents in the chemical method are similar to that of mediators in MER (Rincón-Rodríguez et al. 2024), which makes it possible to compare EEC values measured by the two methods. Meanwhile, microbiological methodologies offer a novel perspective on the bioavailable EEC, and the bioavailable EEC represents the electrons transferred by RAMs that are both spatially and redox-thermodynamically accessible to microorganisms (Saquing et al. 2016). Therefore, the difficulty in comparing the resultant values among the methodologies comes from differences in the probing capabilities caused by the redox potential range and the spatial accessibility of RAMs. Table 2 summarizes the advantages, disadvantages, detection ranges, duration, and applicable scenarios of methods that were relatively frequently used in the previous publications. Moreover, the measured redox properties would not always equal the apparent redox properties in realistic application scenarios. Thus, researchers can select the most appropriate methodology for the application scenarios to make the resultant EEC more comparable.

Different feedstocks were distinguished by dot color, while different references were distinguished using dot shape.

6 Environmental aging induced changes in redox properties

Once biochar enters the environment, the RAMs will undergo structural evolution in response to physicochemical factors. For example, the redox activities of RAMs were pH-dependent, as only phenolic−OH and semiquinone-type PFRs functioned in acidic and neutral conditions, and oxidation by semiquinone-type PFRs and quinoid C=O appeared under alkaline conditions (Zhong et al. 2019). The EAC and EDC of humic substances were also found to increase and decrease, respectively, with increasing natural temperature, which promotes the oxidation and transformation of electron-donating moieties (Tan et al. 2017). During long-term biochar aging, natural rainfall or freeze–thaw events can lead to mechanical fragmentation, release of dissolved organic matter (DOM), mineral dissolution, and surface oxidation (Wang et al. 2020a). Interaction between minerals, microbes, or DOM can also induce pore blockage and increased mineral or functional groups (Wang et al. 2020a; Li et al. 2024b; Hagemann et al. 2017). The aging described above will alter the surface area and chemistry of biochar, thus influencing its EEC and the functions in long-term applications. The aging processes and their effects on EEC are shown in Fig. 5.

6.1 Disintegration and fragmentation

6.1.1 Dissolved black carbon

When exposed to mechanical stress after application, biochar undergoes physical degradation, including

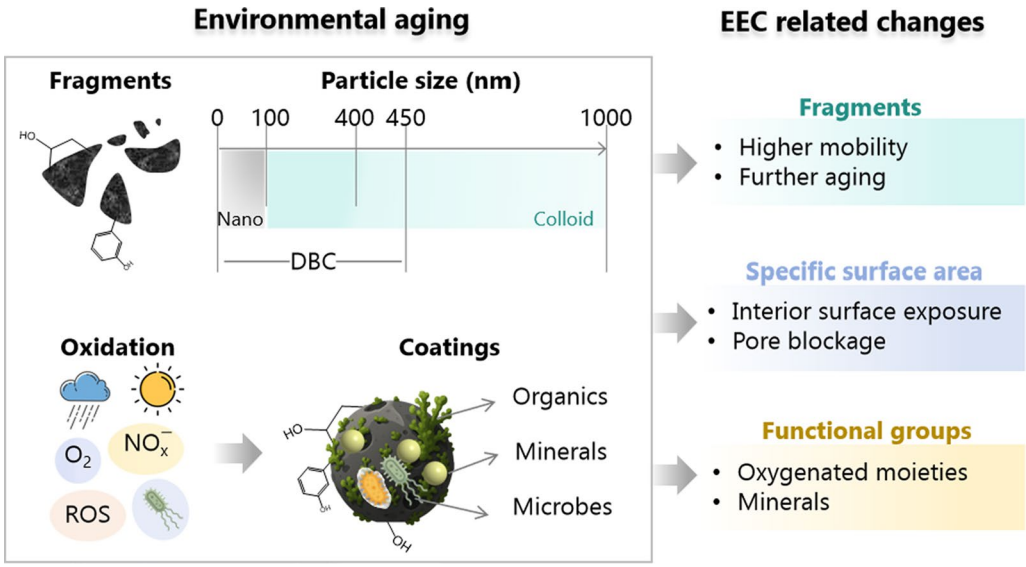

Fig. 5 Environmental aging-induced changes in RAMs and SSA

structural fracturing and fragmentation, leading to the formation of dissolved black carbon (DBC) (Spokas et al. 2014). DBC is operationally defined as biochar with a diameter less than 0.45 μm (Lian and Xing 2024; Qu et al. 2016). Biochar has been estimated to release substantial DBC into the aqueous environment (Dittmar et al. 2012). Structural expansion and shrinkage during rainfall and freeze–thaw cycles are the dominant causes of biochar fragmentation into DBC (Wang et al. 2020a; Zhu et al. 2024; Lian and Xing 2017). The amount and components of DBC are dependent on the feedstock type and biochar formation temperature, as the DBC from grass biochar (ca. 800 μg g^{-1}) is more than that from wood biochar (ca. 300 μg g^{-1}) (Sun et al. 2021), and DBC transfers from saturation/reduction to unsaturation/oxidation of high carbon oxidation states with increasing pyrolysis temperature (Song et al. 2023).

6.1.2 Colloidal and nano-biochar

DBC strictly contains undissolved nanosized biochar and truly dissolved biochar-derived organic fractions (Lian and Xing 2024). Nano-biochar is in the size range of 0–100 nm, and the size of colloidal biochar is defined in the range of 100–1000 nm. However, the individual nanoparticle is only an intermediate state, as nano-biochar tends to form homo- and hetero-aggregates and exhibits high colloidal stability, with particle sizes distributed from ca. 100–400 nm (Lian and Xing 2024; Wang et al. 2019b). Truly dissolved fractions of biochar are mainly composed of condensed aromatic complexes or clusters, and will probably grow into nano-biochar as both colloidal and nano-biochar possess lower Gibbs free energy and higher structural stability than the truly dissolved fractions (Lian and Xing 2024). Nano-biochar was reported to inhibit the replication of resistance genes while only adsorption occurred on bulk biochar (Lian et al. 2020), which indicated the property discrepancy between nano and bulk biochar. Colloidal and nano-biochar were demonstrated to contain higher oxygen content, more negative charges, less carbon and aromatic structure than bulk biochar, and the amorphous fraction in bulk biochar was more readily degraded into nano biochar than the graphitic component (Liu et al. 2018; Qu et al. 2016; Safari et al. 2019). Nano-biochar has a higher external surface area and specific surface area than bulk biochar due to its nanoscale dimensions, which can lead to greater exposure of RAMs(Lian and Xing 2024). Colloidal and nano-biochar are also capable of acting as electron donors and facilitating the reduction of Fe/Mn minerals and Cr(VI) (Wu et al. 2022; Chen et al. 2022b).

6.1.3 EEC evolution

The release of DBC will cause bulk biochar to lose more oxygenated, labile carbon, thereby altering the EECs. Specifically, the EDC and EAC of crop biochar-derived DBC measured by MEO and MER are in the range of 0.02–7.10 mmol e^- g^{-1} C and 0.01–0.81 mmol e^- g^{-1} C, respectively (Zhang et al. 2023, 2019a; Zheng et al. 2019; Xu et al. 2021a), which come from the abundant oxygenated and nitrogenous functional groups in DBC (Sun et al. 2021). The EAC of most DBC falls into the range observed for bulk biochar, while the EDC is significantly higher than that of bulk biochar in Fig. 2 (Mann–Whitney U test, $p < 0.05$), which can be ascribed to the

observation that DBC contains 30–40% more oxygen and more polar functional groups but fewer aromatic clusters than bulk biochar (Qu et al. 2016). DBC has also been proven to act as electron shuttles to mediate the redox cycles, such as the transformation of ferrihydrite (Zhang et al. 2023), Cr(VI), and As(III) (Dong et al. 2014). After DBC is released from bulk biochar, 80–90% of bulk biochar remains as residue biochar, and the carbon and oxygen content of residue biochar will increase by ca. 5–10% compared to bulk biochar (Qu et al. 2016). The undissolved residue biochar was also demonstrated to function as an electron donor and shuttle to boost the biodegradation of pollutants, such as pristine biochar, although the efficiency decreased slightly compared to pristine biochar (Wang et al. 2025), which is critical to the electron transfer functions of biochar in the long term. Furthermore, the EEC evolution of biochar colloids forming from further disintegration of the residue biochar is dependent on the spatial distribution of RAMs in biochar particles, which is decided by pyrolysis mechanisms, such as unreacted-core-shrinking approximation as well as decomposition and condensation (Li et al. 2023).

6.2 Adsorption/coating

On the other hand, mineral and organic coatings will cause blockage and influence the surface chemistry, surface area, pore volume, and pore diameter of biochar (Wang et al. 2020a; Hagemann et al. 2017).

6.2.1 Minerals

Minerals have been observed to both increase and decrease the specific surface area (SSA). Fenton-treatment lowered the SSA of granular activated carbon by 25% due to the Fe-blocked porous structure (Zárate-Guzmán et al. 2019), while Fe minerals infusing into the pore structure of biochar increased SSA and pore volume by 23–43% (Cui et al. 2021), which is probably ascribed to the difference in the labile carbon content of carbonaceous materials and mineral concentration (Jiang et al. 2025; Wang et al. 2020a). As mentioned above (5.2 section), the loading of redox-active minerals can promote the EEC of biochar due to their redox properties and the induced formation of RAMs. Moreover, the Fe–C cycling processes will alter the redox properties of both Fe and organic matter. Fe(II) can generate ROS, degrading or synthesizing organic matter, while organic matter affects the redox properties of Fe by serving in electron transfer or co-precipitation and complexation with Fe (Dong et al. 2023).

6.2.2 Organics

A humic-like organic coating was observed on biochar after co-composting, covering outer and inner (pore) surfaces and adding hydrophilicity, redox-active moieties, and additional mesoporosity of biochar (Hagemann et al. 2017). Humic substances are the most abundant organic matter and account for 70% and 25% of organic matter in soil and groundwater, respectively (Lipczynska-Kochany 2018). Besides, it has been proven that humic/fulvic acid coating increases carboxyl, lactonic, and phenolic groups and decreases surface area and pore volume (Zhao et al. 2019; Wu and Chen 2019). The redox-active DBC will be released from biochar, and redox-active humic substances will simultaneously coat biochar. The EECs of biochar were demonstrated to increase after interactive molecular exchange between humic acid and biochar (Li et al. 2024b).

6.3 Oxidation and degradation

6.3.1 Abiotic oxidation

Abiotic oxidation was suggested to be dominant in biochar oxidation, which can occur via atmospheric oxygen/rainfall-induced oxidation and photochemical transformation (Wang et al. 2020a). Specifically, 2-month atmospheric aging can increase the oxygenated moieties in sludge biochar by 2% (Wang et al. 2017). Dissolved oxygen and nitrogen oxides in rainwater can lead to oxidation. RAMs in DBC and the carbon matrix of biochar can contribute to the formation of ROS, which, in turn, can oxidize biochar through Fenton-like reactions (Fang et al. 2017; Lian and Xing 2024). The chemical oxidation of biochar will introduce negatively charged oxygen-containing functional groups and result in higher mobility and lower PFR concentration (Wang et al. 2019b; Chen et al. 2023).

6.3.2 Microbial degradation

Microbial colonization and degradation will alter biochar properties, such as surface oxidation and the loss of labile carbon, leading to the introduction of oxygenated functional groups and the release of DBC (Wang et al. 2020a; Quan et al. 2020). Fungi can degrade recalcitrant aromatic moieties of biochar (Bamminger et al. 2016), and the breakdown of C=C bonds would lead to the formation of carboxyl, phenolic, and carbonyl groups on the surface (Mia et al. 2017). Although microbial metabolisms can increase the surface functional groups of biochar, microbial coating may also block the pores (Kaudal and Weatherley 2018) and reduce the exposure of RAMs on interior surfaces.

6.4 Comprehensive influences

Overall, disintegration-induced dissolution and pore collapse will expose more internal surfaces, while mineral, organic, and microbial coatings will block the pores (Wang et al. 2020a; Ren et al. 2018; Kaudal and

Weatherley 2018), which can make the SSA and pore volume of aging biochar higher or lower than those of pristine biochar. The SSA and pore volume ratios of aging biochar relative to pristine biochar range from 0.5–2 and 0.01–3.33, respectively (Wang et al. 2020a; Tan et al. 2020). Physical disintegration induced by freeze–thaw, dry–wet cycles, and biotic/abiotic oxidation can introduce more redox-active oxygenated moieties (Tan et al. 2020). However, although the presence of redox-active oxygenated moieties can serve as electron donors or acceptors, the SSA still makes the resulting changes in EECs unpredictable. Besides, the structure and EECs of released DBC are highly dependent on the feedstock, pyrolysis temperature, and the spatial distribution of RAMs in biochar (Sun et al. 2021; Song et al. 2023; Li et al. 2023). Colloidal and nano-biochar have has higher mobility than bulk biochar (Yang et al. 2020), and will subsequently undergo a similar aging process, including chemical oxidation, photooxidation, and biotic transformation (Fu et al. 2016; Lian and Xing 2024; Chen et al. 2022c). Understanding these aging processes is critical for predicting the long-term electron transfer performance of biochar in real environmental systems, as structural and chemical changes directly alter the activity and accessibility of RAMs. However, multiple factors cause opposing effects on RAMs and their accessibility, making the net change in EEC and subsequent performance in electron transfer unpredictable. Therefore, the aging-induced changes in EECs still require further research to better understand the long-term influences of biochar on biogeochemical redox cycles.

7 Targeted enhancement of biochar redox properties

Feedstock selection and preloading, pyrolysis process regulation, and post-treatment of biochar can be effective strategies to enhance the redox properties of biochar (Chacon et al. 2020; Chen et al. 2022a). The EECs vary with feedstocks that introduce different functional moieties (Klüpfel et al. 2014; Li et al. 2020), and pre-loading can introduce heteroatoms, resulting in more redox sites in biochar (Chacon et al. 2020). In pyrolysis processes, changing temperature (Klüpfel et al. 2014; Li et al. 2020), atmosphere (Chen et al. 2025a, 2025b), pyrolysis methods (such as using microwave-assisted pyrolysis (Chen et al. 2022a)), and introducing pyrolysis catalysts (Lü et al. 2022; Chen et al. 2026) can increase the number of RAMs and SSA. Post-treatment with oxidants, acids, alkalis, or UV irradiation, etc., can triple EECs (Chacon et al. 2020), and post-activation with KOH and pyrolysis can achieve an 80-fold increase (Lü et al. 2022) by multiplying oxygenated moieties or SSA. In specific scenarios, modification strategies for biochar may lead to a mutual compensation between EDC and EAC. For example, NaClO oxidizes C–OH into C=O to enhance EAC but decreases EDC (Chacon et al. 2020), which should be carefully considered when designing redox-active biochar.

Nevertheless, the modification processes might result in an unstable structure, increased energy consumption, secondary pollution, and/or additional costs (Zhang et al. 2022). For instance, CO_2 activation and magnesium impregnation could induce the formation of surface oxygen functional groups but decrease the stability of biochar (Xu et al. 2021b; Zhang et al. 2022). KOH activation significantly increased the EEC of biochar, whereas an additional pyrolysis step increased energy input and decreased biochar yield (Lü et al. 2022). Loading with redox-active metals could enhance the redox properties of biochar (Chacon et al. 2020; Cheng et al. 2017), but the release risk of these metals and the resulting pollution cannot be ignored. Fe_3O_4 or MnO_2 coating on biochar could increase its surface area by about 14 times, with the cost rising by 10–20 times accordingly (Zhang et al. 2022; Maneechakr and Mongkollertlop 2020). Therefore, how to regulate feedstocks and preparation processes to maintain the electron-donating and electron-accepting capacities of pristine biochar at a high level, and how to modify biochar to enhance its performance at lower cost and with reduced pollution are the two obstacles to the competitiveness of biochar.

Co-pyrolysis of multiple types of organic waste offers a promising strategy for tailoring the elemental composition and redox-active sites of biochar, which can not only enable the effective utilization of intrinsic elements present in waste streams but also reduce the introduction of secondary pollutants that may arise from conventional activation methods (Chen et al. 2025c). A one-step activation method can also reduce energy consumption by combining pyrolysis and activation processes (Wang et al. 2022b, 2022c). The mass ratio of activator to feedstock, activation temperature, and time can also be optimized to balance biochar properties and cost (Wang et al. 2024b, 2020b). However, the physicochemical properties of biochar become variable and challenging to be finely tuned due to the complexity of feedstock components and the diversity of preparation methods and conditions. Machine learning can effectively predict the properties and capacities of biochar, uncovering underlying reaction mechanisms and complex relationships for material design (Wei et al. 2024a), which has been successfully used for function-oriented biochar design, including advanced oxidation of contaminants (Wang et al. 2024a) and CO_2 capture (Yuan et al. 2024). Moreover, the combination of physics-based modelling and artificial intelligence, which can provide previously missing links among

atomic-scale structure, microscopic properties, and macroscopic functionality of amorphous materials, makes the design of amorphous functional materials promising (Liu et al. 2025). The multitask model makes it possible to balance the functions of biochar and environmental risks or costs (Yin et al. 2024).

8 Conclusions and perspectives

In response to the large-scale application demands for biochar, this review discusses its superior advantages over other analogous functional materials in enhancing extracellular and catalytic electron transfer, highlighting the role of its distinctive redox properties in facilitating the redox reactivity. The roles and accessibility of RAMs in facilitating electron transfer are critically elucidated. The types and spatial distribution of RAMs in biochar and how these characteristics influence EEC are elaborated. Quantitative methods for measuring EEC, including chemical, electrochemical, and microbiological techniques, are detailed, with an emphasis on the respective strengths, limitations, and key considerations. Furthermore, we elucidate the effects of environmental aging on the redox properties of biochar, summarize targeted enhancement strategies of redox properties along with their limitations, and propose prospects for future research.

(1) The inherent RAMs in biochar make redox properties a feature distinguishing it from other analogous functional materials. Meanwhile, compared with granular activated carbon and graphite, biochar outperforms in facilitating extracellular electron transfer, and its catalytic efficiency for abiotic electron transfer rivals that of zero-valent iron, with its redox properties serving as the principal contributors. Moreover, given the low cost and widespread availability of biochar, the capacity to facilitate electron transfer likely represents a promising opportunity for its large-scale application.

(2) The contributions of conductivity and redox properties of biochar to electron transfer and the ROS generated from biochar activation exhibit variability in different scenarios, yet the underlying mechanisms remain unclear. Based on the analysis in this review, we propose that the redox potential difference between RAMs in biochar and electron transfer partners (e.g., microorganisms, oxidants, and reductants) is likely a dominant factor influencing the role of redox properties in electron transfer.

(3) The molecular structures and spatial distribution of RAMs in biochar govern the availability associated with redox potential and spatial accessibility, respectively. Both are critical for elucidating electron-transfer mechanisms and optimizing application effects. However, apart from quinone/hydroquinone and pyridinic-N/pyrrolic-N, the functions of other RAMs remain disputed. Moreover, current techniques for mapping the microscale distribution of RAMs remain scarce and lack broad applicability, requiring further investigation.

(4) Chemical, electrochemical, and microbiological techniques have all been employed to quantify EEC of biochar, but it is essential to standardize the operations to eliminate the specific interferences in practice. Furthermore, since electron-transfer probes (i.e., redox reagents, mediators, and microbes) differ in redox potentials and the spatial accessibilities to RAMs, the resulting EEC values can vary substantially. Consequently, quantitative methods should be selected according to the intended application scenarios to obtain comparable EEC values.

(5) Environmental aging introduces additional oxygenated functional groups onto biochar. Physical disintegration fragments biochar into colloidal and nano-particles, thereby increasing internal surface exposure. Conversely, mineral, organic, and microbial coatings can reduce accessible surface area. These multiple factors make net changes in the EEC of aging biochar difficult to predict. Therefore, monitoring the evolution of structure and redox properties is critical for understanding the long-term performance of biochar in electron transfer.

(6) Precise tuning of biochar properties and the trade-offs among performance, material/energy inputs, and pollution are the two challenges in targeted biochar preparation. Co-pyrolysis of multiple types of organic waste to modulate the interior elements, combined with data-driven multi-objective optimization, offers a promising strategy for targeted enhancement of biochar EEC.

Acknowledgements
Not applicable

Author contributions
Conceptualization: Shasha Li, Fan Lü, Pinjing He; Formal analysis and investigation: Shasha Li, Yanling Ren, Zimeng Zhang; Writing—original draft preparation: Shasha Li; Writing—review and editing: Xiaoying Hu, Zhenhan Duan, Lili Yang, Jianwei Du; Funding acquisition: Shasha Li, Zhenhan Duan, Yong Wen; Resources & Supervision: Mingyang Zhang, Yong Wen.

Funding
This work was supported by the National Natural Science Foundation of China [52400176, 52300168], Chinese Academy of Engineering Sciences Guangdong Institute 2024 Annual Consulting Research Projects [2024-GD-12] and Central Public-interest Scientific Institution Basal Research Fund of China [PM-zx703-202406–170, PM-zx703-202502–019].

Data availability
The datasets generated during and/or analysed during the current study are available from the corresponding author on reasonable request.

Declarations

Competing interests
The authors declare no competing financial interest.

Author details
[1]Ministry of Ecology and Environment, South China Institute of Environmental Sciences, Guangzhou 510530, China. [2]Institute of Waste Treatment and Reclamation, Tongji University, Shanghai 200092, People's Republic of China. [3]State Environmental Protection Key Laboratory of Environmental Pollution Health Risk , Assessment, South China Institute of Environmental Sciences, Ministry of Ecology and Environment, Guangzhou 510530, China.

Received: 4 August 2025 Revised: 3 February 2026 Accepted: 10 February 2026
Published online: 31 March 2026

References

Aeschbacher M, Vergari D, Schwarzenbach RP et al (2011) Electrochemical analysis of proton and electron transfer equilibria of the reducible moieties in humic acids. Environ Sci Technol 45:8385–8394
Ai J, Yin W, B. Hansen HC (2019) Fast dechlorination of chlorinated ethylenes by green rust in the presence of bone char. Environ Sci Technol Lett 6:191–196
Ai J, Ma H, Tobler DJ et al (2020) Bone char mediated dechlorination of trichloroethylene by green rust. Environ Sci Technol 54:3643–3652
Amen R, Bashir H, Bibi I et al (2020) A critical review on arsenic removal from water using biochar-based sorbents: The significance of modification and redox reactions. Chem Eng J 396:125195
Bamminger C, Poll C, Sixt C et al (2016) Short-term response of soil microorganisms to biochar addition in a temperate agroecosystem under soil warming. Agr Ecosyst Environ 233:308–317
Bauer M, Heitmann T, Macalady DL (2007) Electron transfer capacities and reaction kinetics of peat dissolved organic matter. Environ Sci Technol 41:139–145
Bleda-Martínez MJ, Lozano-Castelló D et al (2006) Chemical and electrochemical characterization of porous carbon materials. Carbon 44:2642–2651
Byrne JM, Klueglein N, Pearce C et al (2015) Redox cycling of Fe(II) and Fe(III) in magnetite by Fe-metabolizing bacteria. Science 347:1473
Chacón FJ, Cayuela ML, Roig A et al (2017) Understanding, measuring and tuning the electrochemical properties of biochar for environmental applications. Rev Environ Sci Bio Technol 16:695–715
Chacon FJ, Sanchez-Monedero MA, Lezama L et al (2020) Enhancing biochar redox properties through feedstock selection, metal preloading and post-pyrolysis treatments. Chem Eng J 395:125100
Chen SS, Rotaru AE, Shrestha PM et al (2014) Promoting interspecies electron transfer with biochar. Sci Rep 4:5019
Chen L, Hu J, Han Q et al (2022a) Resolving the enhancement effect of microwave-assisted pyrolysis on biochar redox properties from the structure-activity relationship. J Anal Appl Pyrolysis 167:105706
Chen M, Chen X, Xu X et al (2022b) Biochar colloids facilitate transport and transformation of Cr(VI) in soil: active site competition coupling with reduction reaction. J Hazard Mater 440:129691
Chen Y, Sun K, Sun H et al (2022c) Photodegradation of pyrogenic dissolved organic matter increases bioavailability: novel insight into bioalteration, microbial community succession, and C and N dynamics. Chem Geol 605:120964
Chen X, Gao X, Yu P et al (2023) Rapid simulation of decade-scale charcoal aging in soil: changes in physicochemical properties and their environmental implications. Environ Sci Technol 57:128–138
Chen S, Liu J, Lin Z et al (2025a) Atmosphere-dependent pyrolytic transformability of glass fiber/epoxy resin composites in waste wind turbine blades. Chem Eng J 505:159675
Chen Y, Liu J, Li L et al (2025b) Optimizing pyrolysis of herbal tea and *Salvia miltiorrhiza* residues for sustainable energy and product recovery. Chem Eng J 513:162694
Chen Z, Liu J, Zhuang P et al (2025c) Steering nitrogen and carbon dynamics for functional biochar and emission mitigation via co-pyrolysis of antibiotic-laden sludge and phytoremediation biomass. Chem Eng J 525:169530
Chen Z, Liu J, Tao L et al (2026) Interaction effects of feedstock and temperature on biogas production during torrefaction-coupled catalytic stepwise pyrolysis of phytoremediation biomass. Renew Energy 260:125131
Cheng B-H, Zeng RJ, Jiang H (2017) Recent developments of post-modification of biochar for electrochemical energy storage. Bioresour Technol 246:224–233
Choi C, Ashby DS, Butts DM et al (2020) Achieving high energy density and high power density with pseudocapacitive materials. Nat Rev Mater 5:5–19
Cui L, Fan Q, Sun J et al (2021) Changes in surface characteristics and adsorption properties of 2,4,6-trichlorophenol following Fenton-like aging of biochar. Sci Rep 11:4293
Cuong DV, Wu P-C, Chen L-I et al (2021) Active MnO_2/biochar composite for efficient As(III) removal: insight into the mechanisms of redox transformation and adsorption. Water Res 188:116495
Dhanda A, Raj R, Sathe SM et al (2023) Graphene and biochar-based cathode catalysts for microbial fuel cell: performance evaluation, economic comparison, environmental and future perspectives. Environ Res 231:116143
Ding K, Xu W (2016) Black carbon facilitated dechlorination of DDT and its metabolites by sulfide. Environ Sci Technol 50:12976–12983
Dittmar T, De Rezende CE, Manecki M et al (2012) Continuous flux of dissolved black carbon from a vanished tropical forest biome. Nat Geosci 5:618–622
Dong X, Ma LQ, Gress J et al (2014) Enhanced Cr(VI) reduction and As(III) oxidation in ice phase: important role of dissolved organic matter from biochar. J Hazard Mater 267:62–70
Dong H, Zeng Q, Sheng Y et al (2023) Coupled iron cycling and organic matter transformation across redox interfaces. Nature Reviews Earth & Environment 4:659–673
Du L, Xu W, Liu S et al (2020) Activation of persulfate by graphitized biochar for sulfamethoxazole removal: the roles of graphitic carbon structure and carbonyl group. J Colloid Interface Sci 577:419–430
Fang G, Gao J, Liu C et al (2014) Key role of persistent free radicals in hydrogen peroxide activation by biochar: implications to organic contaminant degradation. Environ Sci Technol 48:1902–1910
Fang G, Liu C, Gao J et al (2015) Manipulation of persistent free radicals in biochar to activate persulfate for contaminant degradation. Environ Sci Technol 49:5645–5653
Fang G, Liu C, Wang Y et al (2017) Photogeneration of reactive oxygen species from biochar suspension for diethyl phthalate degradation. Appl Catal B 214:34–45
Feng N, Meng R, Zu L et al (2019) A polymer-direct-intercalation strategy for MoS2/carbon-derived heteroaerogels with ultrahigh pseudocapacitance. Nat Commun 10:1372
Fu H, Liu H, Mao J et al (2016) Photochemistry of dissolved black carbon released from biochar: reactive oxygen species generation and phototransformation. Environ Sci Technol 50:1218–1226
Gao Y, Sun Y, Song W et al (2023) Intrinsic properties of biochar for electron transfer. Chem Eng J 475:146356
Hagemann N, Joseph S, Schmidt HP et al (2017) Organic coating on biochar explains its nutrient retention and stimulation of soil fertility. Nat Commun 8:1089
He M, Xu Z, Hou D et al (2022) Waste-derived biochar for water pollution control and sustainable development. Nat Rev Earth Environ 3:444–460
Huang C, Qin F, Zhang C et al (2023) Effects of Heterogeneous Metals on the Generation of Persistent Free Radicals as Critical Redox Sites in Iron-Containing Biochar for Persulfate Activation. ACS ES&T Water 3:298–310
Inagaki M, Konno H, Tanaike O (2010) Carbon materials for electrochemical capacitors. J Power Sources 195:7880–7903
Ji J, Zhang H, Zhang F et al (2025) Organic acid promoting the degradation of nonylphenol by persistent free radicals in biochar. Chem Eng J 512:162446

Jiang L, Chen X, Carey GR et al (2025) Effects of physical and chemical aging of colloidal activated carbon on the adsorption of per- and polyfluoroalkyl substances. Environ Sci Technol 59:3691–3702
Kah M, Sigmund G, Xiao F et al (2017) Sorption of ionizable and ionic organic compounds to biochar, activated carbon and other carbonaceous materials. Water Res 124:673–692
Kalinke C, de Oliveira PR, Bonacin JA et al (2021) State-of-the-art and perspectives in the use of biochar for electrochemical and electroanalytical applications. Green Chem 23:5272–5301
Kaudal BB, Weatherley AJ (2018) Agronomic effectiveness of urban biochar aged through co-composting with food waste. Waste Manag 77:87–97
Klüpfel L, Keiluweit M, Kleber M et al (2014) Redox properties of plant biomass-derived black carbon (biochar). Environ Sci Technol 48:5601–5611
Levar CE, Hoffman CL, Dunshee AJ et al (2017) Redox potential as a master variable controlling pathways of metal reduction by *Geobacter sulfurreducens*. ISME J 11:741–752
Li S, Shao L, Zhang H et al (2020) Quantifying the contributions of surface area and redox-active moieties to electron exchange capacities of biochar. J Hazard Mater 394:122541
Li Q, Gao X, Liu Y et al (2021) Biochar and GAC intensify anaerobic phenol degradation via distinctive adsorption and conductive properties. J Hazard Mater 405:124183
Li S, Shao L, Zhang H et al (2022) A nanoscale observation to explain the discrepancy of electron exchange capacities between biochar containing comparable surface redox-active moieties. Biochar 4:41
Li S, Lü F, Zhang H et al (2023) Electron exchange capacities of colloidal biochar: Affected by spatial structure distribution instead of particle size. Chem Eng J 455:140567
Li A, Yao J, Li N et al (2024a) Effect of biochar, graphene, carbon nanotubes, and nanoparticles on microbial denitrification: a review. Crit Rev Environ Sci Technol 7:1–24
Li S, He P, Zhang H et al (2024b) Variations in redox properties of biochar and humic acid induced by interactive molecular exchange. Carbon Res 3(1):26
Li X, Tan M, Wu B et al (2024c) Redox oscillation-driven production of reactive oxygen species from black carbon. Environ Sci Technol 58:21210–21217
Lian F, Xing BS (2017) Black carbon (biochar) in water/soil environments: molecular structure, sorption, stability, and potential risk. Environ Sci Technol 51:13517–13532
Lian F, Xing B (2024) From bulk to nano: formation, features, and functions of nano-black carbon in biogeochemical processes. Environ Sci Technol 58:15910–15925
Lian F, Yu W, Zhou Q et al (2020) Size matters: Nano-biochar triggers decomposition and transformation inhibition of antibiotic resistance genes in aqueous environments. Environ Sci Technol 54:8821–8829
Lipczynska-Kochany E (2018) Humic substances, their microbial interactions and effects on biological transformations of organic pollutants in water and soil: a review. Chemosphere 202:420–437
Liu G, Zheng H, Jiang Z et al (2018) Formation and physicochemical characteristics of nano biochar: insight into chemical and colloidal stability. Environ Sci Technol 52:10369–10379
Liu C-F, Liu Y-C, Yi T-Y et al (2019a) Carbon materials for high-voltage supercapacitors. Carbon 145:529–548
Liu P, Ptacek CJ, Blowes DW et al (2019b) A method for redox mapping by confocal micro-X-ray fluorescence imaging: using Chromium species in a biochar particle as an example. Anal Chem 91:5142–5149
Liu WJ, Jiang H, Yu H-Q (2019c) Emerging applications of biochar-based materials for energy storage and conversion. Energy Environ Sci 12:1751–1779
Liu Y, Madanchi A, Anker AS et al (2025) The amorphous state as a frontier in computational materials design. Nat Rev Mater 10:228–241
Lü C, Shen Y, Li C et al (2020) Redox-active biochar and conductive graphite stimulate methanogenic metabolism in anaerobic digestion of waste-activated sludge: beyond direct interspecies electron transfer. ACS Sustain Chem Eng 8:12626–12636
Lü F, Lu XM, Li SS et al (2022) Dozens-fold improvement of biochar redox properties by KOH activation. Chem Eng J 429:132203
Mai D, Wen R, Cao W et al (2017) Effect of heavy metal (Zn) on redox property of hydrochar produced from lignin, cellulose, and D-xylose. ACS Sustain Chem Eng 5:3499–3508
Maneechakr P, Mongkollertlop S (2020) Investigation on adsorption behaviors of heavy metal ions (Cd2+, Cr3+, Hg2+ and Pb2+) through low-cost/active manganese dioxide-modified magnetic biochar derived from palm kernel cake residue. J Environ Chem Eng 8:104467
Marzbali MH, Hakeem IG, Short G et al (2023) Continuous adsorption of ammonium from primary and digester effluents using biosolids-derived biochar and cation exchange resin. J Water Process Eng 53:103692
Mia S, Dijkstra FA, Singh B (2017) Chapter one - long-term aging of biochar: a molecular understanding with agricultural and environmental implications. Adv Agronomy Acad Press. https://doi.org/10.1016/bs.agron.2016.10.001
Prado A, Berenguer R, Esteve-NúñEZ A (2019) Electroactive biochar outperforms highly conductive carbon materials for biodegrading pollutants by enhancing microbial extracellular electron transfer. Carbon 146:597–609
Prevoteau A, Ronsse F, Cid I et al (2016) The electron donating capacity of biochar is dramatically underestimated. Sci Rep 6:32870
Pu X, Zhao D, Fu C et al (2021) Understanding and calibration of charge storage mechanism in cyclic voltammetry curves. Angew Chem Int Ed Engl 60:21310–21318
Qin C, Wang H, Yuan X et al (2020) Understanding structure-performance correlation of biochar materials in environmental remediation and electrochemical devices. Chem Eng J 382:122977
Qu X, Fu H, Mao J et al (2016) Chemical and structural properties of dissolved black carbon released from biochars. Carbon 96:759–767
Quan G, Fan Q, Zimmerman AR et al (2020) Effects of laboratory biotic aging on the characteristics of biochar and its water-soluble organic products. J Hazard Mater 382:121071
Ratasuk N, Nanny MA (2007) Characterization and quantification of reversible redox sites in humic substances. Environ Sci Technol 41:7844–7850
Ren XH, Wang F, Zhang P et al (2018) Aging effect of minerals on biochar properties and sorption capacities for atrazine and phenanthrene. Chemosphere 206:51–58
Ren S, Usman M, Tsang DCW et al (2020) Hydrochar-facilitated anaerobic digestion: evidence for direct interspecies electron transfer mediated through surface oxygen-containing functional groups. Environ Sci Technol 54(9):5755
RINCÓN-Rodríguez JC, Cárdenas-Hernández PA, Murillo-Gelvez J et al (2024) Comparative evaluation of mediated electrochemical reduction and chemical redox titration for quantifying the electron accepting capacities of soils and redox-active soil constituents. Environ Sci Technol 58:17674–17684
Safari S, von Gunten K, Alam MS et al (2019) Biochar colloids and their use in contaminants removal. Biochar 1:151–162
Saha N, Xin DH, Chiu PC et al (2019) Effect of pyrolysis temperature on acidic oxygen-containing functional groups and electron storage capacities of pyrolyzed hydrochars. ACS Sustain Chem Eng 7:8387–8396
Sander M, Hofstetter TB, Gorski CA (2015) Electrochemical analyses of redox-active iron minerals: a review of nonmediated and mediated approaches. Environ Sci Technol 49:5862–5878
Saquing JM, Yu YH, Chiu PC (2016) Wood-derived black carbon (biochar) as a microbial electron donor and acceptor. Environ Sci Technol Lett 3:62–66
Sathishkumar K, Li Y, Sanganyado E (2020) Electrochemical behavior of biochar and its effects on microbial nitrate reduction: role of extracellular polymeric substances in extracellular electron transfer. Chem Eng J 395:125077
Sevilla M, Mokaya R (2014) Energy storage applications of activated carbons: supercapacitors and hydrogen storage. Energy Environ Sci 7:1250–1280
Shao L, Li S, Cai J et al (2019) Ability of biochar to facilitate anaerobic digestion is restricted to stressed surroundings. J Clean Prod 238:117959
Shi L, Dong H, Reguera G et al (2016) Extracellular electron transfer mechanisms between microorganisms and minerals. Nat Rev Microbiol 14:651–662
Song F, Li T, Wu F et al (2023) Temperature-dependent molecular evolution of biochar-derived dissolved black carbon and its interaction mechanism with polyvinyl chloride microplastics. Environ Sci Technol 57:7285–7297
Spokas KA, Novak JM, Masiello CA et al (2014) Physical disintegration of biochar: an overlooked process. Environ Sci Technol Lett 1:326–332
Srividhya G, Ponpandian N (2024) Pseudocapacitance: mechanism and characteristics. In: Gupta RK (ed) Pseudocapacitors: fundamentals to

high performance energy storage devices. Springer Nature Switzerland, Cham, pp 39–56. https://doi.org/10.1007/978-3-031-45430-1_3
Su X, Wang X, Ge Z et al (2024) KOH-activated biochar and chitosan composites for efficient adsorption of industrial dye pollutants. Chem Eng J 486:150387
Sun T, Levin BDA, Guzman JJL et al (2017) Rapid electron transfer by the carbon matrix in natural pyrogenic carbon. Nat Commun 8:14873
Sun T, Levin BDA, Schmidt MP et al (2018) Simultaneous Quantification of Electron Transfer by Carbon Matrices and Functional Groups in Pyrogenic Carbon. Environ Sci Technol 52:8538–8547
Sun Y, Xiong X, He M et al (2021) Roles of biochar-derived dissolved organic matter in soil amendment and environmental remediation: a critical review. Chem Eng J 424:130387
Tan G, Yu H-Q (2023) Rethinking biochar: black gold or not? Nat Rev Mater. https://doi.org/10.1038/s41578-023-00634-1
Tan WB, Xi BD, Wang GA et al (2017) Increased electron-accepting and decreased electron-donating capacities of soil humic substances in response to increasing temperature. Environ Sci Technol 51:3176–3186
Tan L, Ma Z, Yang K et al (2020) Effect of three artificial aging techniques on physicochemical properties and Pb adsorption capacities of different biochars. Sci Total Environ 699:134223
Tao W, Zhang P, Li H et al (2022) Generation mechanism of persistent free radicals in lignocellulose-derived biochar: roles of reducible carbonyls. Environ Sci Technol 56:10638–10645
Tian R, Dong H, Chen J et al (2021) Electrochemical behaviors of biochar materials during pollutant removal in wastewater: a review. Chem Eng J 425:130585
Wang J, Wang S (2019) Preparation, modification and environmental application of biochar: a review. J Clean Prod 227:1002–1022
Wang H, Feng M, Zhou F et al (2017) Effects of atmospheric ageing under different temperatures on surface properties of sludge-derived biochar and metal/metalloid stabilization. Chemosphere 184:176–184
Wang GJ, Gao X, Li Q et al (2019a) Redox-based electron exchange capacity of biowaste-derived biochar accelerates syntrophic phenol oxidation for methanogenesis via direct interspecies electron transfer. J Hazardous Mater 390:121726
Wang Y, Zhang W, Shang J et al (2019b) Chemical aging changed aggregation kinetics and transport of biochar colloids. Environ Sci Technol 53:8136–8146
Wang L, O'connor D, Rinklebe J et al (2020a) Biochar aging: mechanisms, physicochemical changes, assessment, and implications for field applications. Environ Sci Technol 54:14797–14814
Wang X, Zeng W, Liu W et al (2020b) CO2 adsorption of lignite chars after one-step KOH activation. New J Chem 44:13755–13763
Wang J, Cai J, Wang S et al (2022a) Biochar-based activation of peroxide: multivariate-controlled performance, modulatory surface reactive sites and tunable oxidative species. Chem Eng J 428:131233
Wang X, Zeng W, Kong X et al (2022b) Development of low-cost porous carbons through alkali activation of crop waste for CO2 capture. ACS Omega 7:46992–47001
Wang X, Zeng WL, Xin CL et al (2022c) The development of activated carbon from corncob for CO2 capture. RSC Adv 12:33069–33078
Wang X, Zhang P, Wang C et al (2022d) Metal-rich hyperaccumulator-derived biochar as an efficient persulfate activator: role of intrinsic metals (Fe, Mn and Zn) in regulating characteristics, performance and reaction mechanisms. J Hazard Mater 424:127225
Wang M, Ren T, Yin M et al (2023a) Enhanced anaerobic wastewater treatment by a binary electroactive material: pseudocapacitance/conductance-mediated microbial interspecies electron transfer. Environ Sci Technol 57:12072–12082
Wang R, Zhang S, Chen H et al (2023b) Enhancing biochar-based nonradical persulfate activation using data-driven techniques. Environ Sci Technol 57:4050–4059
Wang R, Chen H, He Z et al (2024a) Discovery of an end-to-end pattern for contaminant-oriented advanced oxidation processes catalyzed by biochar with explainable machine learning. Environ Sci Technol 58:16867–16876
Wang X, Kong F, Zeng W et al (2024b) The Resource Utilization of Poplar Leaves for CO2 Adsorption. Molecules 29:2024
Wang S, Han J, Ge Z et al (2025) Mechanistic insight into enhancement of undissolved rice husk biochar on tetracycline biodegradation by strain *Serratia marcescens* basing on electron transfer response. J Hazard Mater. https://doi.org/10.1016/j.jhazmat.2025.137895
Wei X, Liu Y, Shen L et al (2024a) Machine learning insights in predicting heavy metals interaction with biochar. Biochar 6:10
Wei X, Zhang X, Jin L et al (2024b) Waste biomass-derived biochar in adsorption-photocatalytic conversion of CO_2 for sustainable energy and environment: evaluation, mechanism, and life cycle assessment. Appl Catal B: Environ Energy 351:123957
Wu YJ, Chen BL (2019) Effect of fulvic acid coating on biochar surface structure and sorption properties towards 4-chlorophenol. Sci Total Environ 691:595–604
Wu S, Fang GD, Wang YJ et al (2017) Redox-active oxygen-containing functional groups in activated carbon facilitate microbial reduction of ferrihydrite. Environ Sci Technol 51:9709–9717
Wu S, Cai X, Liao Z et al (2022) Redox properties of nano-sized biochar derived from wheat straw biochar. RSC Adv 12:11039–11046
Xie J, Latif J, Yang K et al (2024) A state-of-art review on the redox activity of persistent free radicals in biochar. Water Res 255:121516
Xin DH, Xian MH, Chiu PC (2019) New methods for assessing electron storage capacity and redox reversibility of biochar. Chemosphere 215:827–834
Xin D, Barkley T, Chiu PC (2020) Visualizing electron storage capacity distribution in biochar through silver tagging. Chemosphere 248:125952
Xin D, Saha N, Reza MT et al (2021) Pyrolysis creates electron storage capacity of black carbon (biochar) from lignocellulosic biomass. ACS Sustain Chem Eng 9:6821–6831
Xu W, Dana KE, Mitch WA (2010) Black carbon-mediated destruction of nitroglycerin and RDX by hydrogen sulfide. Environ Sci Technol 44:6409–6415
Xu W, Pignatello JJ, Mitch WA (2013) Role of black carbon electrical conductivity in mediating hexahydro-1,3,5-trinitro-1,3,5-triazine (RDX) transformation on carbon surfaces by sulfides. Environ Sci Technol 47:7129–7136
Xu X, Huang H, Zhang Y et al (2019) Biochar as both electron donor and electron shuttle for the reduction transformation of Cr(VI) during its sorption. Environ Pollut 244:423–430
Xu W, Walpen N, Keiluweit M et al (2021a) Redox properties of pyrogenic dissolved organic matter (pyDOM) from biomass-derived chars. Environ Sci Technol 55:11434–11444
Xu Z, He M, Xu X et al (2021b) Impacts of different activation processes on the carbon stability of biochar for oxidation resistance. Bioresour Technol 338:125555
Xu Z, Wan Z, Sun Y et al (2022) Electroactive Fe-biochar for redox-related remediation of arsenic and chromium: distinct redox nature with varying iron/carbon speciation. J Hazard Mater 430:128479
Xu H, Hei S, Fu W et al (2025) Unraveling the trade-off effect of pyrogenic carbons between biopseudocapacitors and bioconductors during anaerobic methanogenesis. Environ Sci Technol 59:2861–2874
Yan Y, Ma X, Cao W et al (2018) Identifying the reducing capacity of biomass derived hydrochar with different post-treatment methods. Sci Total Environ 643:486–495
Yang F, Sun L, Xie W et al (2017) Nitrogen-functionalization biochars derived from wheat straws via molten salt synthesis: An efficient adsorbent for atrazine removal. Sci Total Environ 607–608:1391–1399
Yang W, Shang J, Li B et al (2020) Surface and colloid properties of biochar and implications for transport in porous media. Crit Rev Environ Sci Technol 50:2484–2522
Yang H, Chen N, Yang K et al (2025) Microscale spatiotemporal variation of reactive oxygen species in the charosphere: Underlying formation mechanism and their role in CO_2 emission. Environ Sci Technol 59:2095–2106
Yin M, Zhang X, Li F et al (2024) Multitask deep learning enabling a synergy for cadmium and methane mitigation with biochar amendments in paddy soils. Environ Sci Technol 58:1771–1782
Yu W, Lian F, Cui G et al (2018) N-doping effectively enhances the adsorption capacity of biochar for heavy metal ions from aqueous solution. Chemosphere 193:8–16
Yu W, Chu C, Chen B (2022) Enhanced microbial ferrihydrite reduction by pyrogenic carbon: impact of graphitic structures. Environ Sci Technol 56:239–250
Yuan HY, Ding LJ, Zama EF et al (2018) Biochar modulates methanogenesis through electron syntrophy of microorganisms with ethanol as a substrate. Environ Sci Technol 52:12198–12207

Yuan J, Wen Y, Dionysiou DD et al (2022a) Biochar as a novel carbon-negative electron source and mediator: electron exchange capacity (EEC) and environmentally persistent free radicals (EPFRs): a review. Chem Eng J (1996) 429:132313

Yuan J, Wen Y, Dionysiou DD et al (2022b) Biochar as a novel carbon-negative electron source and mediator: electron exchange capacity (EEC) and environmentally persistent free radicals (EPFRs): a review. Chem Eng J. https://doi.org/10.1016/j.cej.2021.132313

Yuan X, Suvarna M, Lim JY et al (2024) Active learning-based guided synthesis of engineered biochar for CO_2 capture. Environ Sci Technol 58:6628–6636

ZáRATE-Guzmán AI, González-Gutiérrez LV, Godínez LA et al (2019) Towards understanding of heterogeneous Fenton reaction using carbon-Fe catalysts coupled to in-situ H2O2 electro-generation as clean technology for wastewater treatment. Chemosphere 224:698–706

Zhang Y, Xu XY, Cao LZ et al (2018) Characterization and quantification of electron donating capacity and its structure dependence in biochar derived from three waste biomasses. Chemosphere 211:1073–1081

Zhang B, Zhou S, Zhou L et al (2019a) Pyrolysis temperature-dependent electron transfer capacities of dissolved organic matters derived from wheat straw biochar. Sci Total Environ 696:133895

Zhang X, Xia J, Pu J et al (2019b) Biochar-mediated anaerobic oxidation of methane. Environ Sci Technol 53:6660–6668

Zhang Y, Xu XY, Zhang PY et al (2019c) Pyrolysis-temperature depended quinone and carbonyl groups as the electron accepting sites in barley grass derived biochar. Chemosphere 232:273–280

Zhang P, Duan W, Peng H et al (2022) Functional Biochar and Its Balanced Design. ACS Environmental Au 2:115–127

Zhang P, Meng X, Liu A et al (2023) Biochar-derived dissolved black carbon accelerates ferrihydrite microbial transformation and subsequent imidacloprid degradation. J Hazard Mater 446:130685

Zhao J, Liang G, Zhang X et al (2019) Coating magnetic biochar with humic acid for high efficient removal of fluoroquinolone antibiotics in water. Sci Total Environ 688:1205–1215

Zhao C, Shao B, Yan M et al (2021) Activation of peroxymonosulfate by biochar-based catalysts and applications in the degradation of organic contaminants: A review. Chem Eng J 416:128829

Zheng X, Liu Y, Fu H et al (2019) Comparing electron donating/accepting capacities (EDC/EAC) between crop residue-derived dissolved black carbon and standard humic substances. Sci Total Environ 673:29–35

Zhong DL, Jiang Y, Zhao ZZ et al (2019) pH dependence of arsenic oxidation by rice-husk-derived biochar: Roles of redox-active moieties. Environ Sci Technol 53:9034–9044

Zhu S, Huang X, Yang X-B et al (2020) Enhanced transformation of Cr(VI) by heterocyclic-N within Nitrogen-doped biochar: Impact of surface modulatory persistent free radicals (PFRs). Environ Sci Technol 54(13):8123

Zhu D, Wang Z, Liu K et al (2023) Multi-cycle anaerobic digestion of hydrothermal liquefaction aqueous phase: Role of carbon and iron based conductive materials in inhibitory compounds degradation, microbial structure shaping, and interspecies electron transfer regulation. Chem Eng J 454:140019

Zhu L, Chen N, Zhang X et al (2024) Freeze–thaw cycle events enable the deep disintegration of biochar: release of dissolved black carbon and its structural-dependent carbon sequestration capacity. Environ Sci Technol 58:20979–20989

Zhu X, Zhou E, Tai X et al (2025) G-C3N4 S-scheme homojunction through Van der Waals interface regulation by intrinsic polymerization tailoring for enhanced photocatalytic H2 evolution and CO2 reduction. Angew Chem Int Ed 64:e202425439